Electronic supplementary information (ESI)

Crystalline-state chemiluminescence reactions of two-fluorophore-linked adamantylideneadamantane 1,2-dioxetane isomers accompanied by solid-to-solid phase transitions

Chihiro Matsuhashi,[a] Hironaga Oyama,[b] Hidehiro Uekusa,[b] Ayana Sato-Tomita,[c] Kouhei Ichiyanagi,[d] Shojiro Maki [a] and Takashi Hirano* [a]

[a] *Department of Engineering Science, Graduate School of Informatics and Engineering, The University of Electro-Communications, Chofu, Tokyo 182-8585, Japan*

[b] *Department of Chemistry, Tokyo Institute of Technology, Ookayama 2-12-1, Meguro-ku, Tokyo, 152-8551, Japan*

[c] *Division of Biophysics, Department of Physiology, Jichi Medical University, Shimotsuke, Tochigi 329-0498, Japan*

[d] *Institute of Materials Structure Science, High Energy Accelerator Research Organization (KEK), Tsukuba, Ibaraki, 305-0801, Japan*

Table of contents

1. General methods

CL spectra were measured with a Hamamatsu Photonics PMA-12 spectrophotometer for UV/visible measurement (C10027) (exposure time: 10 s for heating at 160 °C and 60 s for heating at 130 °C). Sample weights were c.a. 0.5 mg. Melting points were measured with a Yanaco MP-500P, whose heating stage was also used for CL measurements. IR spectra were measured with a JASCO FT/IR-4600 with an ATR attachment. High-resolution mass spectra (HRMS) were obtained with a JEOL JMS-T100LC mass spectrometer for electro-spray ionization (ESI) and a JEOL JMS-S300 mass spectrometer for matrix assisted laser desorption ionization (MALDI) using *trans*-2-[3-(4-*tert*-butylphenyl)-2-methyl-2-propenylidene]malononitrile (DCTB) with NaI and α-cyano-4-hydroxycinnamic acid (CHCA) as matrices. ^{1}H and ^{13}C NMR spectra were recorded on a JEOL ECA-500 instrument (500 MHz for ^{1}H and 126 MHz for ^{13}C). Fluorescence spectra were measured with a Hamamatsu Photonics Quantaurus-QY absolute PL quantum yields measurement system with determining fluorescence quantum yields. Fluorescence life times were measured with a Hamamatsu Photonics Quantaurus-TauC11367. For crystal structure determination, single crystals of *cis*-*syn*-**1**, *cis*-*anti*-**1** and *trans*-**1** were obtained by a vapor diffusion technique using solutions in dichloromethane as a good solvent and *n*-hexane as a poor solvent. Unfortunately, the crystallography of *cis*-*anti*-**1** and *trans*-**1** were not successful. The crystal of *cis*-*anti*-**1** was fiber crystal. It wasn't possible to obtain that of *trans*-**1** because of its instability. Single crystal X-ray diffraction data for *cis*-*syn*-**1** was collected on beamline NW12A with PILATUS3 S 2M at the Photon Factory (Tsukuba, Japan) with synchrotron radiation (λ = 0.750 Å). Single crystal X-ray diffraction data for **2** was collected on a Rigaku XtaLAB AFC10 diffractometer with Mo Kα radiation (λ = 0.71073 Å). The data were collected at 95 K for *cis*-*syn*-**1** and at 100 K for **2**. XDS[1] was used for *cis*-*syn*-**1** and CrysAlisPro 1.171.42.35a (Rigaku Oxford Diffraction, 2021) was used for **2** to perform empirical absorption correction using spherical harmonics, implemented scaling algorithms in CORRECT and SCALE3 ABSPACK, respectively. The single crystal structure of **2** was solved by OLEX2[2] software program. The initial structures were solved by dual space algorithm implemented in *SHELXT*[3] and refined on F_0^2 with *SHELXL*-2017/1 for *cis*-*syn*-**1** and *SHELXL*-2018/3 for **2**.[4] All of the non-hydrogen atoms were refined anisotropically. Hydrogen atoms were geometrically generated and refined with a riding model and their displacement parameters (U_{iso}) were fixed to $1.2U_{eq}$ of the parent carbon atom. The single crystal of *cis*-*syn*-**1** was found to contain solvent molecules. Several peaks could not be assigned to any molecules due to a disorder. PLATON/SQUEEZE[5] method was used to treat a solvent disorder volume, which removed the contributions of some 366 electrons from the unit-cell contents. Crystallographic data are summarized in Table S5. CCDC 2132563 and 2128839 contains the supplementary crystallographic data for this paper (*cis*-*syn*-**1** and **2**, respectively). These data can be obtained free of charge from The Cambridge Crystallographic Data Centre via www.ccdc.cam.ac.uk/structures. Synchrotron powder X-ray diffraction data of *cis*-*syn*-**1** and *cis*-*anti*-**1** were recorded on beamline NW12A with PILATUS3 S 2M at the Photon Factory (Tsukuba, Japan). The crystals of *cis*-*syn*-**1** and *cis*-*anti*-**1** were gently ground and enclosed in Lindemann borosilicate glass capillaries (ϕ 0.5 mm), that were fixed to a brass pin of a sample holder with an epoxy glue. The

sample holder was attached to a goniometer and slowly rotated. The crystal samples were rotated at 2 rpm and heated by N_2 gas flow heated at 130 or 160 °C with collecting X-ray diffraction data. 60 Diffraction images were collected during the measurement of each sample, and the exposure time was set to 30 seconds. Density functional theory (DFT) calculations were performed with the Gaussian 16 program (Rev. D.01).[6] DFT includes the B3LYP function with the 6-31G(d) basis set.[7-9] The molecular structures of all compounds were optimized by DFT calculations, to give information on the ground state structures and the molecular orbitals. Using the optimized structures, time-dependent (TD)-DFT calculations were carried out to give the properties of the electronic transitions including the $S_0 \rightarrow S_1$ transitions. Molecular graphics were made with GaussView, Version 6.1.[10] Thermogravimetry-differential thermal analysis (TG-DTA) of *cis-syn*-**1** was measured with a Rigaku TG8120. Pictures of the single crystals of *cis-syn*-**1** were taken by a digital camera of an optical microscope and dimensions of the crystals were determined with the ImageJ software. A morphological change of a heated single crystal of *cis-syn*-**1** was also taken by the digital camera every 2 s. CL emission from a heated single crystal of *cis-syn*-**1** was observed with a sCMOS camera (exposure time: 20s) attached to the optical microscope. A heating stage for observing a morphological change and CL emission of a heated single crystal of *cis-syn*-**1** was a MSA factory PN121-D controlled its temperature by a MSA factory PCC100G.

2. Synthesis

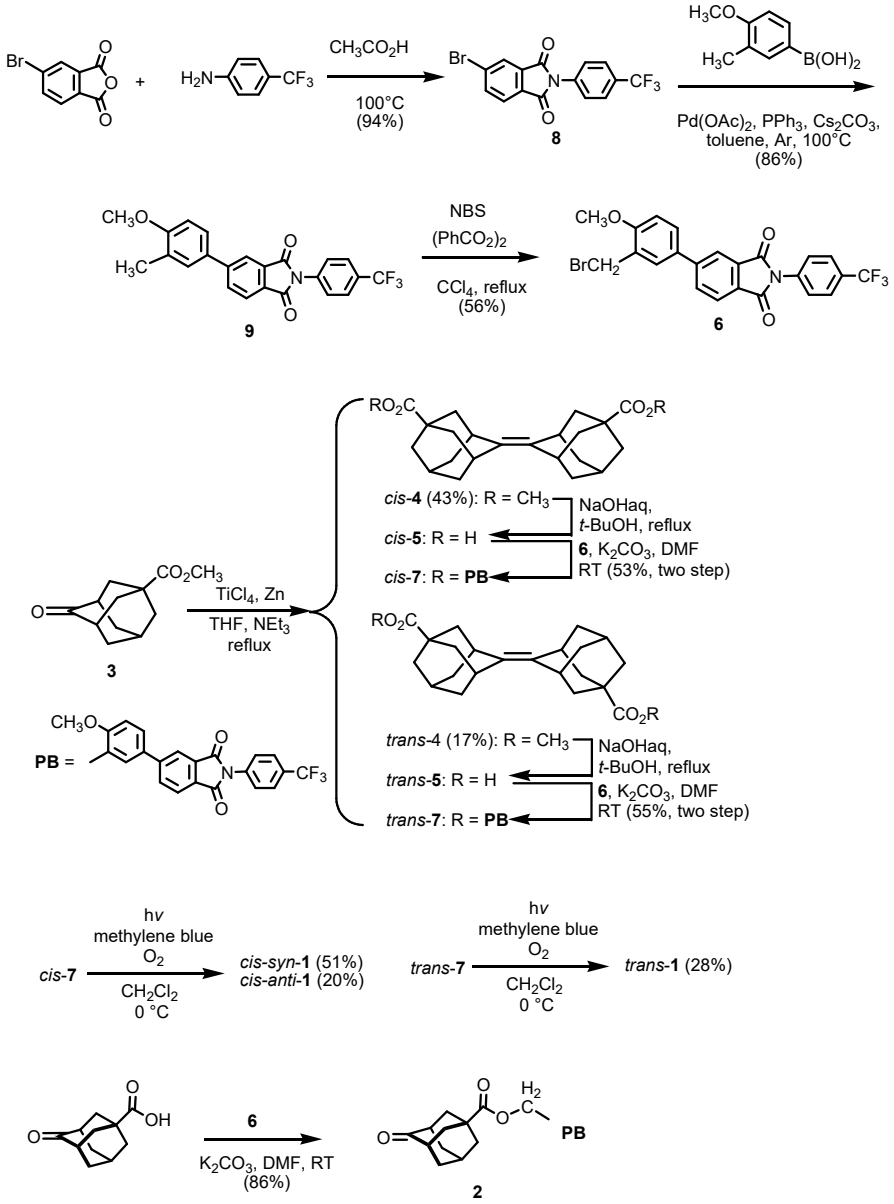

Scheme S1. Synthesis of the two-fluorophore-linked 1,2-dioxetanes **1** and 2-adamantanone **2**.

*5-Bromo-2-[4-(trifluoromethyl)phenyl]isoindoline-1,3-dione (**8**)*.[11] A solution of 4-bromophthalic anhydride (10.1 g, 44.6 mmol) and 4-trifluoromethyanilne (6.9 mL, 54.9 mmol) in acetic acid (100 mL) was heated at 100 ºC under Ar for 4.5 h. The reaction mixture was cooled and diluted with water to make white precipitates of the product. The precipitates were collected by vacuum filtration, washed with water and dried in vacuo, to give phthalimide **8** (15.5 g, 42.0 mmol, 94 %) as colorless powder. ^{1}H NMR (500 MHz, $CDCl_3$) δ 8.12 (d, J = 1.7 Hz, 1 H), 7.97 (dd, J = 8.0, 1.7 Hz, 1 H), 7.85 (d, J = 8.0 Hz, 1 H), 7.78 (d, J = 8.0 Hz, 2 H), 7.63 (d, J = 8.6 Hz, 2 H). *m/z* (MALDI, CHCA) Found: 369.9679 and 371.9661 ($[M+H]^+$). $C_{15}H_8F_3NO_2{}^{79}Br$ and $C_{15}H_8F_3NO_2{}^{81}Br$ require 369.9685 and 371.9666, respectively.

*5-(3-Methyl-4-methoxyphenyl)-2-[4-(trifluoromethyl)phenyl]isoindoline-1,3-dione (**9**).* Palladium (II) acetate (124 mg, 0.55 mmol), triphenyl phosphine (702 mg, 2.68 mmol) and cesium carbonate (8.72 g, 26.8 mmol) were added to a solution of phthalimide **8** (5.04 g, 13.6 mmol) and 4-methoxy-3-methyphenylboronic acid (2.69g, 16.2 mmol) in toluene (250 mL). The solution was heated at reflux for 3 h under Ar. The reaction mixture was cooled and diluted with $CHCl_3$ and the filtrate was extracted with $CHCl_3$ (150 mL × 2) from the aqueous layer, and the organic layer was washed with brine (175 mL), dried over Na_2SO_4 and concentrated in vacuo. The product was subjected to separation by silica gel column chromatography [*n*-hexane/$CHCl_3$ (from 1:1 to 1:3)], to give **9** (4.81 g, 11.7 mmol, 86 %) as colorless powder. mp 227−228 °C. ^{1}H-NMR (500 MHz, $CDCl_3$) δ 8.15 (s, 1 H), 7.99 (d, J = 1.1 Hz, 2 H), 7.79 (d, J = 8.6 Hz, 2 H), 7.67 (d, J = 8.6 Hz, 2 H), 7.51 (m, 2 H), 6.96 (d, J = 8.0 Hz, 1 H), 3.91 (s, 3 H) and 2.32 (s, 3 H). ^{13}C-NMR (126 MHz, $CDCl_3$) δ 166.97, 166.79, 158.83, 148.13, 135.06, 132.50, 132.36, 130.60, 129. 7 (q), 129.60, 128.91, 127.74, 126.44, 126.22 (q), 125.95, 124.83 (q), 124.42, 121.83, 110.43, 55.51 and 16.43. ν/cm^{-1} 3200-2800 (w), 1777, 1708, 1606, 1514, 1382, 1324 and 1110. *m/z* (ESI) Found: 434.0980 ([M+Na]$^+$). $C_{22}H_{16}F_3NO_3$ requires 434.1024.

*5-(3-Bromomethyl-4-methoxyphenyl)-2-[4-(trifluoromethyl)phenyl]isoindoline-1,3-dione (**6**).* A solution of phthalimide **9** (4.43 g, 10.8 mmol), NBS (2.52 g, 14.0 mmol) and benzoyl peroxide (251 mg, 0.54 μmol) in CCl_4 (550 mL) was heated at reflux for 8.5 h under Ar. The reaction was quenched by addition of a saturated sodium thiosulfate solution (300 mL) and the organic layer was washed with brine (200mL). The product was extracted with $CHCl_3$ (300 mL) from the aqueous layer, and the organic layer was washed with brine (200 mL). All of organic layer was dried over Na_2SO_4 and concentrated in vacuo. The product was subjected to separation by silica gel column chromatography [*n*-hexane/$CHCl_3$ (from 1:1 to 1:5)], to give **6** (2.95 g, 6.03 mmol, 56 %) as pale yellow powder. mp 221.7−222.2 °C. ^{1}H-NMR (500 MHz, $CDCl_3$) δ 8.14 (s, 1 H), 8.01 (d, J = 6.9 Hz, 1 H), 7.98 (dd, J = 7.7, 1.4 Hz, 1 H), 7.79 (d, J = 8.6 Hz, 2 H), 7.66-7.68 (m, 3 H), 7.63 (dd, J = 8.6, 2.3 Hz, 1 H), 7.03 (d, J = 8.6 Hz, 1 H), 4.63 (s, 2 H) and 3.97 (s, 3 H). ^{13}C-NMR (126 MHz, $CDCl_3$) δ 166.80, 166.64, 158.30, 147.23, 134.97, 132.60, 132.42, 131.14, 129.82, 129.77 (q), 129.32, 129.10, 127.20, 126.42, 126.23 (q), 124.52, 123.81 (q), 121.86, 111.67, 55.92 and 28.29. ν/cm^{-1} 3100-2850(w), 1777, 1707, 1606, 1513, 1385, 1323, 1124 and 1112. *m/z* (ESI) Found: 490.0247 and 492.0225 ([M+H]$^+$). $C_{23}H_{16}F_3NO_3{}^{79}$Br and $C_{23}H_{16}F_3NO_3{}^{81}$Br require 490.0266 and 492.0245, respectively.

cis- And trans-5,5'-dicarbomethoxyadamantylideneadamantanes (cis- and *trans-**4**)*. $TiCl_4$ (9.0 mL, 82 mmol) was added dropwise to anhydrous THF (160 mL) containing powdered zinc (10.8 g, 165 mmol) in an ice bath under Ar. After heating the mixture under reflux for 1.5 h, triethylamine (22 mL, 158 mmol) was added to the titanium-zinc mixture and stirring at 5 min, following a solution of 5-(merthoxycarbonyl)-2-adamantanone[12,13] (7.4 g, 35.5 mmol) in anhydrous THF (45 mL) was added and the solution was refluxed under Ar for 19 h. The reaction was quenched by the addition of a 10% K_2CO_3 aqueous solution (250 mL), and precipitates were filtered off and washed with ethyl acetate

(200 mL × 3). The filtrate was washed with brine (100 mL × 3), dried over Na_2SO_4 and concentrated in vacuo. The product was purified by silica gel column chromatography (1:5 ethyl acetate/*n*-hexane to ethyl acetate), to yield alkene *cis*-**4** (2.94 g, 7.65 mmol, 43 %, R_f = 0.38) as colorless needles and alkene *trans*-**4** (1.15 g, 2.99 mmol, 17%, R_f = 0.21) as colorless powder.

cis-**4**. mp 134.6−135.4 °C. ^{1}H-NMR (500 MHz, $CDCl_3$) δ 3.65 (s, 6 H), 3.00 (s, 4 H), 2.08 (quint, J = 3.3 Hz, 2 H), 1.96 (m, 8 H), 1.82 (m, 8 H) and 1.66 (m, 4 H). ^{13}C-NMR (126 MHz, $CDCl_3$) δ 177.88, 132.26, 51.60, 40.97, 40.46, 38.42, 31.42 and 28.23. ν/cm^{-1} 2922, 2898, 2850, 1724, 1689, 1448, 1435, 1233, 1182 and 1072. *m/z* (ESI) Found: 407.2190 ([M+Na]$^+$). $C_{24}H_{32}O_4Na$ requires 407.2198.

trans-**4**. mp 209.3−210.3 °C. ^{1}H-NMR (500 MHz, $CDCl_3$) δ 7.26 (s, 1 H), 3.65 (s, 6 H), 3.00 (s, 4 H), 2.07 (qt, J = 2.9 Hz, 2 H), 1.97 (m, 8 H), 1.82 (m, 8 H) and 1.65 (m, 4 H). ^{13}C-NMR (126 MHz, $CDCl_3$) δ 177.89, 132.26, 51.61, 40.99, 40.52, 38.42, 38.36, 31.42, 28.21. ν/cm^{-1} 2951, 1908, 2848, 1720, 1433, 1247 and 1074. *m/z* (ESI) Found: 407.2166 ([M+Na]$^+$). $C_{24}H_{32}O_4Na$ requires 407.2198.

*cis-5,5'-Dicarboxyadamantylideneadamantane (cis-**5**)*. A 1.0 M NaOH aqueous solution (10 mL) was added to a solution of *cis*-**4** (1.12 g, 2.91 mmol) in *t*-BuOH (30 mL), and the resulting mixture was heated at 100°C for 5 h. After removing the solvents, a 1 M HCl aqueous solution was added to the residue in an ice bath. White precipitates were collected by filtration, washed with water and vacuum dried, to give *cis*-**5** (1.55 g) as a crude powder product. Because a ^{1}H-NMR spectrum of the product showed the signals of *cis*-**5** without any impurity, we directly used the product for the next reaction. mp 300 °C (decomp.). ^{1}H-NMR (500 MHz, DMSO-d_6) δ 11.98 (brs, 1 H), 2.96 (brs, 4 H), 2.02 (brs, 2 H), 1.90 (m, 8 H), 1.77 (m, 4 H), 1.70 (m, 4 H) and 1.57 (m, 4 H). ^{13}C-NMR (126 MHz, DMSO-d_6) δ 178.00, 131.78, 132.37, 40.19, 39.98, 39.81, 39.65, 39.49, 37.94, 37.80, 30.75 and 27.56. ν/cm^{-1} 3200-2400 (br, w), 2905, 2849, 1686, 1445, 1288, 1262, 1087 and 956. *m/z* (ESI) Found: 355.1881 ([M−H]$^-$). $C_{22}H_{27}O_4$ requires 355.1909.

*trans-5,5'-Dicarboxyadamantylideneadamantane (trans-**5**)*. A 1.0 M NaOH aqueous solution (10 mL) was added to a solution of *trans*-**4** (622 mg, 1.62 mmol) in *t*-BuOH (25 mL), and the resulting mixture was heated at 100°C for 4.5 h. After removing the solvents, a 1 M HCl aqueous solution was added to the residue in an ice bath. White precipitates were collected by filtration, washed with water and vacuum dried, to give *trans*-**5** (514 mg, 1.44 mmol, 89%) as colorless powder. mp 300 °C (decomp.). ^{1}H-NMR (500 MHz, DMSO-d_6) δ 12.01 (brs, 1 H), 2.96 (brs, 4 H), 2.02 (brs, 2 H), 1.89 (m, 8 H), 1.77 (m, 4 H) and 1.57 (m, 4 H). ^{13}C-NMR (126 MHz, DMSO-d_6) δ 178.00, 131.79, 40.19, 39.99, 39.82, 39.65, 39.39, 37.95, 37.90, 30.75 and 27.56. ν/cm^{-1} 3200-2250 (br, w), 2902, 2847, 1683, 1445, 1412, 1088 and 953. *m/z* (ESI) Found: 355.1860 ([M−H]$^-$). $C_{22}H_{27}O_4$ requires 355.1909.

*cis-5,5'-Di{1-methoxy-4-[4-(trifluoromethyl)phenyl]isoindoline-1,3-dionylbenzyloxycarbonyl} adamantylideneadamantane (cis-**7**)*. A solution of *cis*-**5** (260 mg, crude), bromide **7** (392 mg, 0.80

mmol) and K_2CO_3 (282 mg, 2.04 mmol) in anhydrous DMF (25 mL) was stirred at room temperature for 30 h under Ar. The solution was diluted with water (150 mL) and the product was extracted with the mixed solvent (1:4 ethyl acetate/*n*-hexane, 180 mL × 4). The organic layer was washed with brine (45 mL × 4), dried over Na_2SO_4 and concentrated in vacuo. The crude product was purified by silica gel flush chromatography (from 76:24 to 55:45 ethyl acetate/*n*-hexane), to yield alkene precursor *cis*-**7** (301 mg, 53%) as colorless powder. mp 132.7−133.4 °C. ^{1}H-NMR (500 MHz, $CDCl_3$) δ 8.09 (s, 2 H), 7.97 (d, J = 8.0 Hz, 2 H), 7.93 (dd, J = 8.0, 1.7 Hz, 2 H), 7.77 (d, J = 8.6 Hz, 5 H), 7.65 (d, J = 8.0 Hz, 5 H), 7.59-7.62 (m, 4 H), 6.99 (d, J = 8.0 Hz, 2 H), 5.19 (s, 4 H), 3.89 (s, 6 H), 3.02 (s, 4 H), 2.10 (s, 2 H), 2.03 (d, J = 12.6 Hz, 8 H), 1.87 (m, 4 H), 1.82 (m, 4 H) and 1.66 (m, 4 H). ^{13}C-NMR (126 MHz, $CDCl_3$) δ 177.03, 166.77, 166.66, 158.24, 147.64, 135.01, 132.46, 132.39, 132.27, 130.72, 129.71 (q), 129.13, 128.14, 127.82, 126.38, 126.19 (q), 125.92, 124.47, 123.81(q), 121.76, 111.04, 61.15, 55.67, 41.12, 40.47, 38.48, 38.45, 31.41 and 28.21. ν/cm^{-1} 2903, 2848, 1776, 1715, 1607, 1515, 1365, 1322, 1117, 1065 and 1019. *m/z* (MALDI, DCTB-NaI) Found: 1197.3728 ([M+Na]$^+$). $C_{68}H_{56}F_6N_2O_{10}Na$ requires 1197.3731.

*trans-5,5'-Di{1-methoxy-4-[4-(trifluoromethyl)phenyl]isoindoline-1,3-dionylbenzyloxycarbonyl} adamantylideneadamantane (trans-**7**)*. A solution of *trans*-**5** (67 mg, 0.19 mmol), bromide **7** (155 mg, 0.32 mmol) and K_2CO_3 (117 mg, 0.84 mmol) in anhydrous DMF (10 mL) was stirred for 30 h at room temperature under Ar. The solution was diluted with water (25 mL) and the product was extracted with $CHCl_3$ (40 mL × 4). The organic layer was washed with brine (50 mL × 2), dried over Na_2SO_4 and concentrated in vacuo. The crude product was purified by silica gel column chromatography (1:50 ethyl acetate /$CHCl_3$), to yield alkene precursor *trans*-**7** (108 mg, 58%) as colorless powder. mp 131.3−135.3 °C. ^{1}H-NMR (500 MHz, $CDCl_3$) δ 8.14 (s, 2 H), 8.00 (d, J = 7.4 Hz, 2 H), 7.97 (dd, J = 7.7, 1.4 Hz, 2 H), 7.78 (d, J = 8.0 Hz, 4 H), 7.62-7.67 (m, 8 H), 7.02 (d, J = 9.2 Hz, 2 H), 5.21 (s, 4 H), 3.92 (s, 6 H), 3.02 (brs, 4 H), 2.08 (brs, 2 H), 2.03 (brs, 6 H), 1.89 (brs, 4 H), 1.80 (brs, 4 H) and 1.64 (brs, 4 H). ^{13}C-NMR (126 MHz, $CDCl_3$) δ 177.08, 166.80, 166.69, 158.28, 147.75, 135.00, 132.54, 132.44, 132.27, 130.80, 129.77 (q), 129.18, 128.20, 127.91, 126.41, 126.23 (q), 125.95, 124.49, 123.80 (q), 121.85, 111.06, 61.20, 55.69, 53.43, 41.14, 40.52, 38.48, 38.37, 31.41 and 28.20. ν/cm^{-1} 2903, 2850, 1777, 1715, 1608, 1516, 1365, 1322, 1117, 1065 and 1019. *m/z* (MALDI, DCTB-NaI) Found: 1197.3725 ([M+Na]$^+$). $C_{68}H_{56}F_6N_2O_{10}Na$ requires 1197.3731.

*cis-syn- And cis-anti-5,5'-di{1-methoxy-4-[4-(trifluoromethyl)phenyl]isoindoline-1,3-dionyl-benzyloxycarbonyl}adamantylideneadamantane 1,2-dioxetane (cis-syn-**1** and cis-anti-**1**)*. A solution of *cis*-**7** (300 mg, 0.26 mmol) and methylene blue (3.7 mg, 12 μmol) in dichloromethane (350 mL) was cooled at 0 °C under O_2 and irradiated with a 48 W LED lamp for 5 h. The solution was concentrated in vacuo. A ^{1}H-NMR spectrum of the residue indicated that 49 mg of unreacted *cis*-**7** was recovered and conversion yields of *cis-syn*-**1** and *cis-anti*-**1** were 51 and 20%, respectively. The products were separated by silica gel column chromatography (from 1:50 to 1:20 ethyl acetate /CH_2Cl_2), to give *cis-syn*-**1** (42.4 mg, R_f = 0.30, 1:50 ethyl acetate /CH_2Cl_2) as colorless powder and

cis-anti-**1** (10 mg, R_f = 0.41, 1:50 ethyl acetate /CH_2Cl_2) as a colorless powder. Crystal samples were obtained by recrystallization from dichloromethane and *n*-hexane and stored at −20 °C in a freezer.

cis-syn-**1**. ^{1}H-NMR (500 MHz, $CDCl_3$) δ 8.12 (d, J = 1.1 Hz, 2 H), 8.00 (d, J = 8.0 Hz, 2 H), 7.96 (dd, J = 8.0, 1.7 Hz, 2 H), 7.78 (d, J = 8.0 Hz, 4 H), 7.66 (d, J = 8.6 Hz, 4 H), 7.59-7.63 (m, 4 H), 7.01 (d, J = 8.6 Hz, 2 H), 5.20 (s, 4 H), 3.91 (s, 6 H), 2.75 (brs, 4 H), 2.17-2.21 (m, 4 H), 2.08 (brs, 2 H), 1.92 (brs, 8 H) and 1.78-1.83 (brs, 8 H). ^{13}C-NMR (126 MHz, $CDCl_3$) δ 176.25, 166.82, 166.69, 158.31, 147.70, 135.04, 132.62, 132.43, 130.84, 129.75(q), 129.19, 128.29, 128.04, 126.43, 126.21(q), 125.74, 124.55, 123.82(q), 121.86, 111.08, 94.33, 61.39, 55.69, 39.56, 38.60, 34.06, 33.57, 31.67 and 26.41. ν/cm^{-1} 2927, 2862, 1777, 1717, 1614, 1361, 1323, 1115, 1076, 1065, 836 and 742. *m/z* (MALDI, DCTB-NaI) Found: 1229.3632 ([M+Na]$^+$). $C_{68}H_{56}F_6N_2O_{12}Na$ requires 1229.3630.

cis-anti-**1**. ^{1}H-NMR (500 MHz, $CDCl_3$) δ 7.97 (d, J = 7.4 Hz, 1 H), 7.92 (d, J = 0.9 Hz, 1 H), 7.79 (d, J = 8.6 Hz, 2 H), 7.76 (dd, J = 1.4, 7.7 Hz, 1 H), 7.64 (d, J = 8.0 Hz, 2 H), 5.27 (s, 2 H), 2.77 (brs, 2 H), 2.65 (brs, 2 H), 2.18−2.22 (m, 2 H), 1.84−1.99 (m, 14 H), 1.78 (brs, 1 H), 1.73 (brs, 2 H) and 1.57−1.60 (m, 4 H). ^{13}C-NMR (126 MHz, $CDCl_3$) δ 176.17, 166.67, 166.57, 158.22, 147.46, 134.92, 132.46, 132.33, 130.70, 129.75 (q), 129.12, 128.26, 127.99, 127.03, 126.34, 126.19 (q), 125.58, 124.39, 122.78 (q), 121.67, 120.54, 111.03, 94.61, 61.41, 55.66, 39.95, 38.54, 36.19, 31.64, 31.49 and 26.18. ν/cm^{-1} 2939, 2914, 2860, 1779, 1712, 1613, 1511, 1379, 1322, 1114, 1085, 1064, 021, 839 and 745. *m/z* (MALDI, DCTB-NaI) Found: 1229.3635 ([M+Na]$^+$). $C_{68}H_{56}F_6N_2O_{12}Na$ requires 1229.3630.

*trans-5,5'-Di{1-methoxy-4-[4-(trifluoromethyl)phenyl]isoindoline-1,3-dionyloxycarbonyl}adamantylideneadamantane 1,2-dioxetane (trans-**1**)*. A solution of alkene *trans*-**7** (300 mg, 0.26 mmol) and methylene blue (3.7 mg, 12 μmol) in dichloromethane (350 mL) was cooled at 0 °C under O_2 and irradiated with a 48 W LED lamp for 5 h. The solution was concentrated in vacuo. The products were separated by silica gel column chromatography (from 1:50 to 1:10 ethyl acetate /CH_2Cl_2), to yield *trans*-**1** (22 mg, conversion yield 28%) as a colorless powder with unreacted *trans*-**7** (43 mg)). Crystal samples were obtained by recrystallization from dichloromethane and *n*-hexane and stored at −20 °C in a freezer.

^{1}H-NMR (500 MHz, $CDCl_3$) δ 8.13 (s, 2H), 8.01 (d, J = 8.0 Hz, 2 H), 7.95-7.98 (m, 2 H), 7.76-7.79 (m, 4 H), 7.59-7.67 (m, 8 H), 7.02 (t, J = 8.9 Hz, 2 H), 5.22 (s, 2 H), 5.19 (s, 2 H), 3.91 (s, 3 H), 3.90 (s, 3 H), 2.73 (brs, 4 H), 2.17 (brs, 4 H), 1.87-2.01 (m, 12 H), 1.76 (brs, 4 H) and 1.52-1.58 (brs, 2 H). ν/cm^{-1} 2933, 2864, 1777, 1715, 1608, 1367, 1322, 1117, 1065, 1019, 837 and 744. *m/z* (MALDI, DCTB-NaI) Found: 1229.3635 ([M+Na]$^+$). $C_{68}H_{56}F_6N_2O_{12}Na$ requires 1229.3630. ^{13}C-NMR couldn't measure because *trans*-**1** is unstable and decomposes over time.

*5-{1-Methoxy-4-[4-(trifluoromethyl)phenyl]isoindoline-1,3-dionylbenzyloxycarbonyl}-2-adamantanone (**2**)*. A solution of 5-carboxy-2-adamantanone (52 mg, 0.27 mmol), bromide **6** (123 mg, 0.25 mmol), and potassium carbonate (77 mg, 0.56 mmol) in anhydrous DMF (5 mL) was stirred at room temperature for 4 h under Ar. The reaction mixture was diluted by adding water (20 mL),

and the product was extracted with ethyl acetate (90 mL × 3). The organic layer was washed with brine (35 mL × 3), dried over Na_2SO_4 and concentrated in vacuo. The product was purified by silica gel flush chromatography (from 32:68 to 53:47 ethyl acetate / *n*-hexane), to yield **2** (130 mg, 0.22 mmol, 86%) as colorless powder. mp 195.3−196.1 °C. ^{1}H-NMR (500 MHz, $CDCl_3$) δ 8.14 (d, J = 1.1 Hz, 1 H), 8.02 (d, J = 7.4 Hz, 1 H), 7.97 (dd, J = 7.4, 1.7 Hz, 1 H), 7.79 (d, J = 8.6 Hz, 2 H), 7.67 (d, J = 9.0 Hz, 2 H), 7.65 (dd, J = 8.0, 2.5Hz, 1 H), 7.60 (d, J = 2.9 Hz, 1 H), 7.04 (d, J = 8.6 Hz, 1 H), 5.24 (s, 2 H), 3.92 (s, 3 H), 2.60 (brs, 2 H), 2.21-2.27 (m, 5 H), 2.17 (brs, 2 H), 2.04-2.07 (m, 2 H) and 1.99 (brs, 2 H). ^{13}C-NMR (126 MHz, $CDCl_3$) δ 216.67, 175.52, 166.83, 166.67, 158.48, 147.59, 134.98, 132.60, 132.47, 130.92, 129.80 (q), 129.27, 128.64, 128.52, 126.44, 126.23 (q), 125.33, 124.57, 123.81 (q), 121.89, 111.20, 61.88, 55.73, 45.78, 40.52, 40.17, 38.32, 37.86 and 27.28. ν/cm^{-1} 2926, 2862, 1774, 1716, 1603, 1518, 1360, 1320, 1116 and 1064. *m/z* (ESI) Found: 626.1786 ($[M+H]^+$). $C_{34}H_{28}F_3NO_6Na$ requires 626.1766.

3. Reaction analysis of the thermal decompositions of *cis-syn*-**1** and *cis-anti*-**1** in the crystalline state

A crystal samples of *cis-syn*-**1** (2.7 mg) was heated at 130 °C for 1.0 h. Similarly, a crystal sample of *cis-anti*-**1** (1.6 mg) was heated at 160 °C for 1.0 h. To each sample, 1.0 μL of mesitylene (7.2 μmol) was added as an internal standard, and the sample was dissolved in $CDCl_3$. Then, ^{1}H NMR spectra of the solutions were measured. Consumed amounts of *cis-syn*-**1** and *cis-anti*-**1** were estimated with the integral values of the signals at δ 5.20 ppm (s, 4 H) for *cis-syn*-**1** and δ 5.11 ppm (s, 4 H) for *cis-anti*-**1** relative to that at δ 6.80 ppm (s, 3 H) for mesitylene (Table S1). The crystal sample of *cis-syn*-**1** contained 0.7 molecule of CH_2Cl_2 and 0.3 molecule of *n*-hexane for each *cis-syn*-**1** molecule as observed by a ^{1}H-NMR measurement. Representative ^{1}H NMR spectra were shown in Figures S1 and S2, indicating the quantitative productions of **2** by the thermal decompositions of *cis-syn*-**1** and *cis-anti*-**1**.

Table. S1 Analyses of thermal decompositions of *cis-syn*-**1** (130℃, 3.0 h) and *cis-anti*-**1** (160℃, 1.0 h) in the crystalline state.

1,2-dioxetane	amount of the substrate		percentage of consumption (%)
	before heating ($\times 10^{-6}$ mol)	after heating ($\times 10^{-6}$ mol)	
cis-syn-**1**	2.21	1.78	19.5
cis-anti-**1**	1.29	0.84	34.8

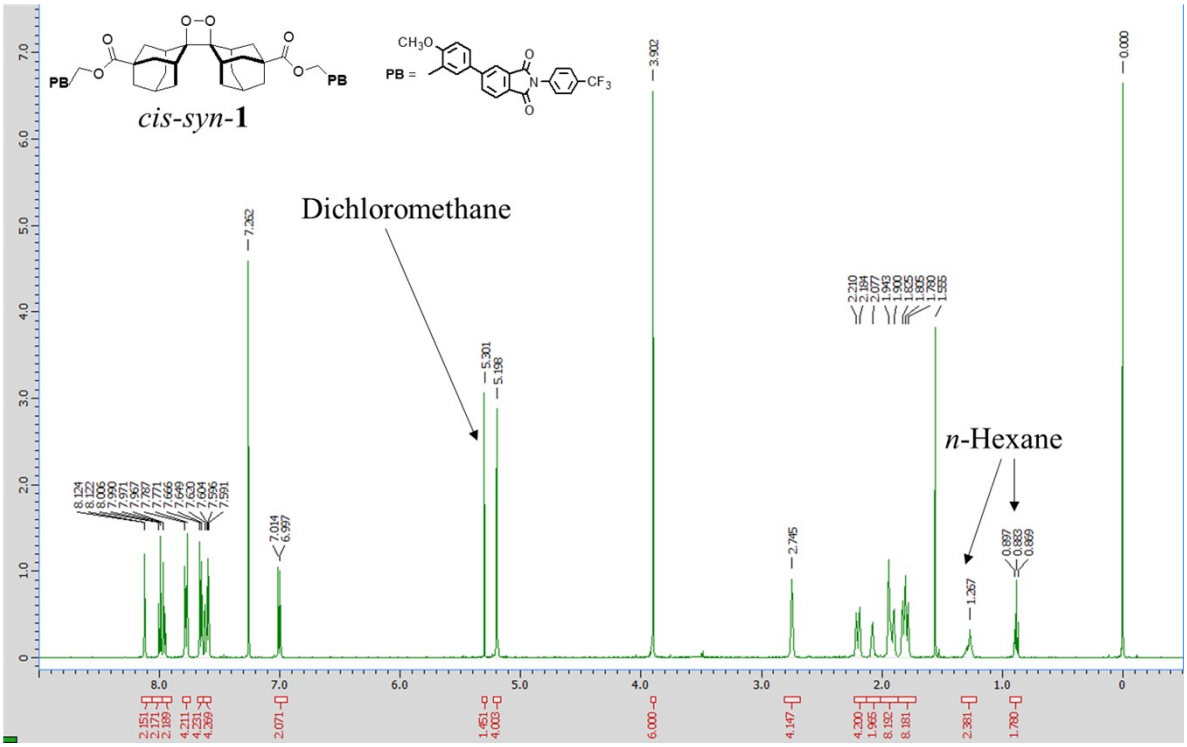

Fig. S1 ^{1}H NMR spectrum of a solution of *cis-syn*-**1** in $CDCl_3$ before heating.

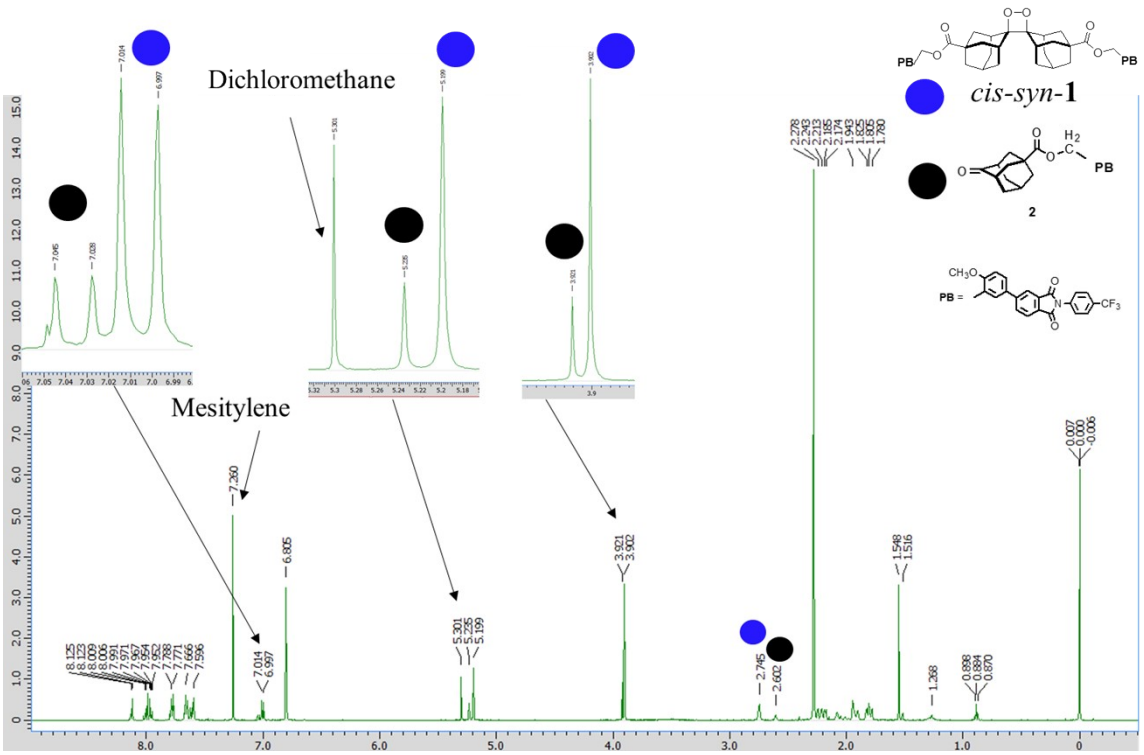

Fig. S2 ^{1}H NMR spectrum (in $CDCl_3$) of the reaction mixture obtained by heating the crystal sample of *cis-syn*-**1** at 130 ºC for 3.0 h.

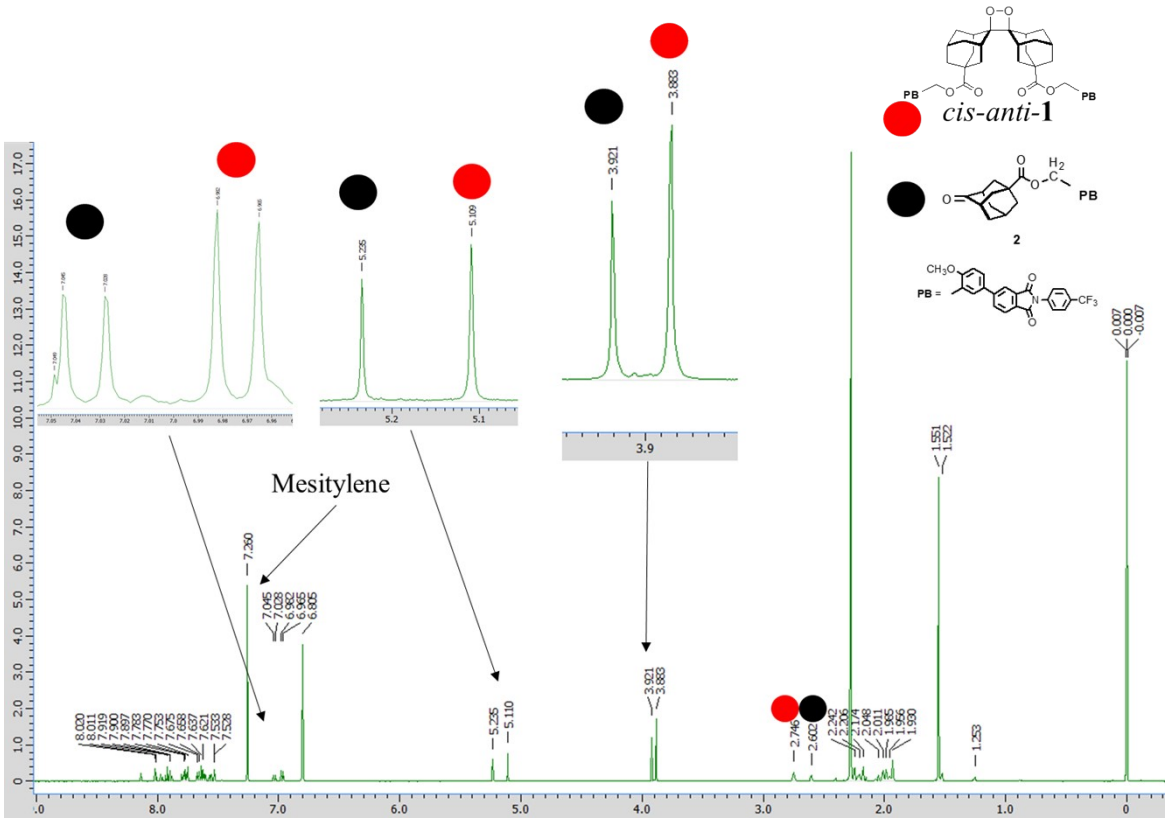

Fig. S3 ^{1}H NMR spectrum (in $CDCl_3$) of the reaction mixture obtained by heating the crystal sample of *cis-anti*-**1** at 160 ºC for 1.0 h.

4. Time course changes of CL emission intensities and morphological changes for the crystals of *cis-syn*-1 heated at 130 °C

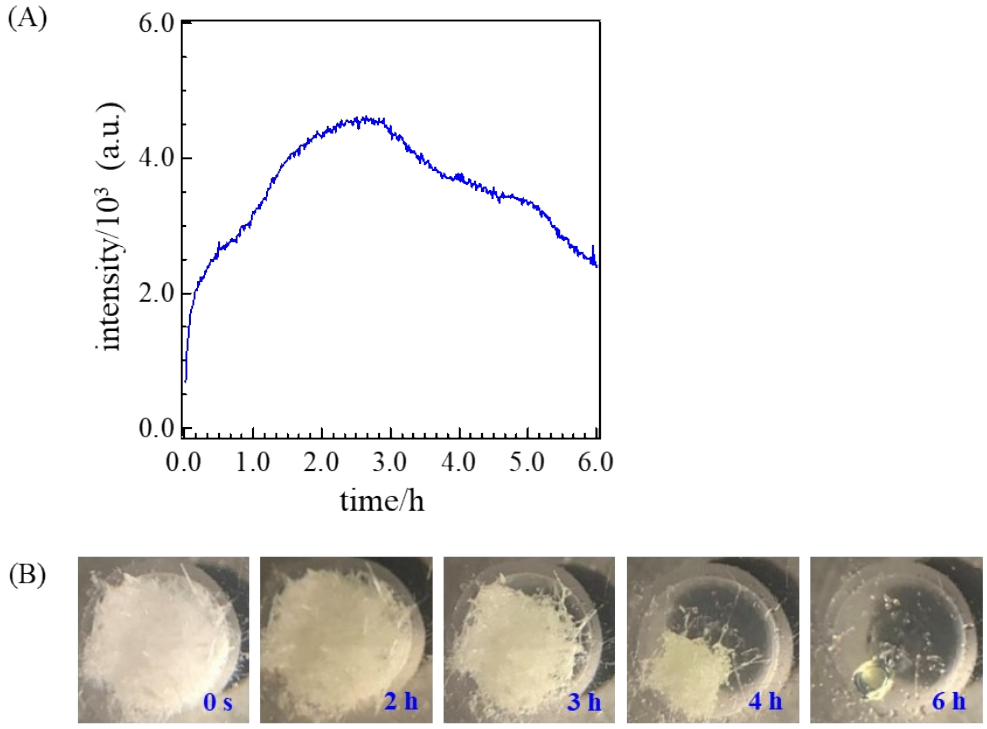

Fig. S4 (A) Time course changes of CL emission intensities observed for the crystal samples of *cis-syn*-**1** heated at 130 °C (monitored at 461 nm). (B) Morphological changes of a heated crystal sample of *cis-syn*-**1**. Times after the starts of heating were shown in the pictures.

5. Fluorescence of fluorophore-linked 2-adamantanone 2, *cis-syn*-1 and cis-*anti*-1

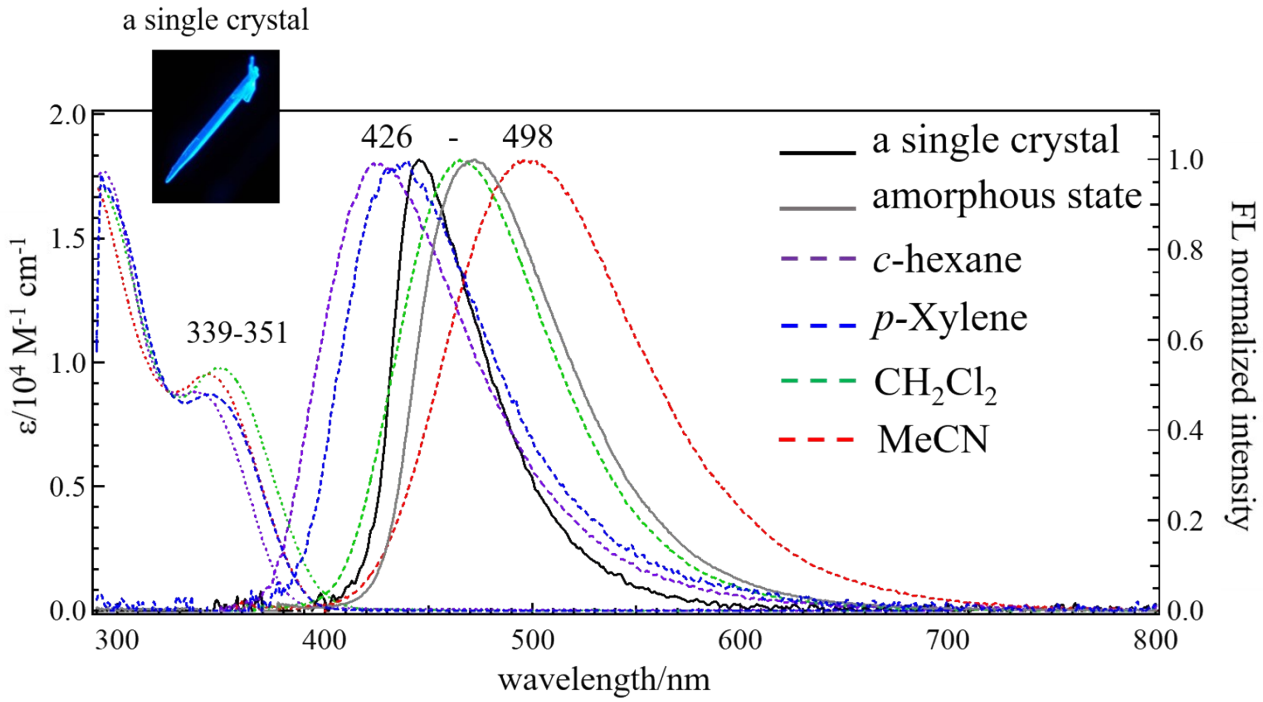

Fig. S5 Fluorescence spectra of **2** with samples in solutions (cyclohexane, *p*-xylene, CH_2Cl_2 and acetonitrile) and solid states (crystalline and amorphous states) at 298 K.

Table S2. Fluorescence properties of **2** at 298 K.

solvent ($E_T(30)^a$) or solid state	λ_{abs}/nm (ε /10^3 M^{-1} cm^{-1})^b	λ_f/nm (Φ_f) [λ_{ex} / nm]^c
MeCN (45.6)	344 (9.56)	498 (0.96) [350]
CH_2Cl_2 (40.7)	351 (9.79)	465 (1.0) [350]
p-xylene (34.3)	344 (8.72)	436 (0.10) [350]
c-hexane (30.8)	339 (8.83)	426 (0.12) [350]
a single crystal	-	445 (0.52) [380]
amorphous state	-	470 (0.66) [380]

[a] Solvent parameter $E_T(30)$ in kcal mol^{-1}.

[b] Absorption maxima (λ_{abs}) and molar absorption coefficient (ε) in parenthesis.

[c] Emission maxima (λ_{fl}), quantum yield (Φ_f) in parenthesis and excitation wavelength (λ_{ex}) in square bracket.

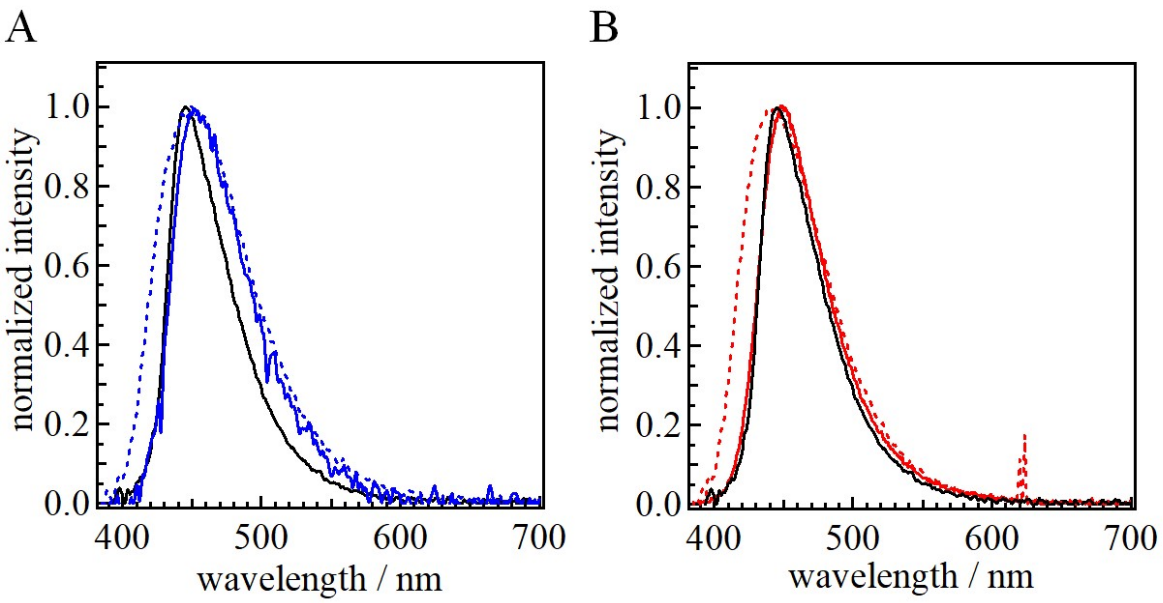

Fig. S6 Comparison of the emission spectra of the crystalline-state CL of *cis-syn*-**1** (A, blue solid line) and *cis-anti*-**1** (B, red solid line) with the crystalline-state fluorescence spectra of **2** (black solid line), *cis-syn*-**1** (A, blue dashed line) and *cis-anti*-**1** (B, red dashed line).

Table S3. Fluorescence properties of *cis-syn*-**1** and *cis-anti*-**1** in the crystalline state at 298 K.

compound	λ_f/nm (Φ_f) [λ_{ex} = 380 nm][a]
cis-syn-**1**	449 (0.38)
cis-anti-**1**	440 (0.36)

[a]Emission maximum (λ_{fl}), quantum yield (Φ_f) in parenthesis and excitation wavelength (λ_{ex}) in square bracket.

6. Fluorescence lifetime measurements of fluorophore-linked 2-adamantanone 2

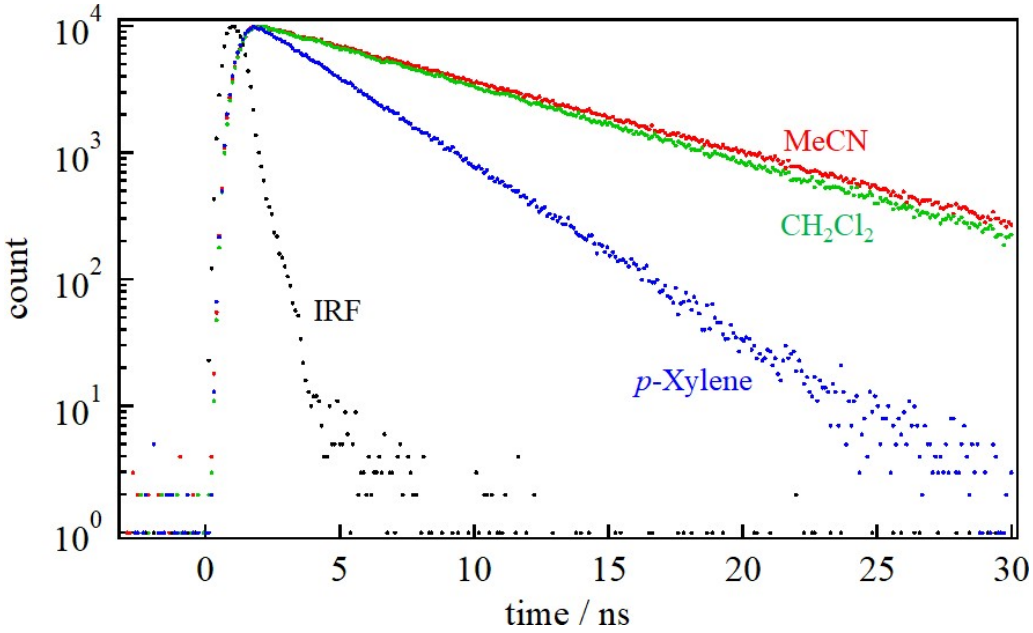

Fig. S7 Fluorescence lifetime measurements of **2** in *p*-xylene, CH_2Cl_2 and acetonitrile.

Table S4. Fluorescence lifetimes and rate constants of the fluorescence emission process for **2** at 298 K.

solvent ($E_T(30)$ [a])	τ_f [b]/ns	k_f [c]/10^8 s^{-1}
MeCN (45.6)	7.67	1.28
CH_2Cl_2 (40.7)	7.14	1.40
p-xylene (34.3)	3.08	0.33

[a] Solvent parameter $E_T(30)$ in kcal mol^{-1}.

[b] Fluorescence lifetime.

[c] Rate constant of the fluorescence emission process determined by $k_f = \Phi_f \tau_f^{-1}$.

7. X-ray crystallographic analyses of *cis-syn*-1 and 2

Table S5. Crystal data and structure refinement for *cis-syn*-**1** and **2**.

	cis-syn-**1**	**2**
CCDC deposit code	2132563	2128839
Formula	C_{68} H_{56} F_6 N_2 O_{12}	C_{34} H_{28} F_3 N O_6
Formula weight	1207.14	603.57
T / K	95(2)	100
Wavelength / Å	0.750	0.71075
Crystal system	monoclinic	monoclinic
Space group	$P2_1/c$	$P\bar{1}$
a / Å	28.409(15)	7.4930(4)
b / Å	17.899(6)	13.8284(10)
c / Å	12.633(5)	15.4815(13)
α / °	90	108.781(7)
β / °	101.158(18)	101.858(6)
γ / °	90	105.672(6)
V / Å^3	6302(5)	1384.96(19)
Z	4	2
D_{calc} / g cm^{-3}	1.272	1.447
μ / mm^{-1}	0.099	0.112
F(000)	2512	628.0
Reflections collected	43430	25797
Independent reflections	6588	6970
Refined parameters	796	426
GOF on F^2	1.025	1.054
R_1 [$I > 2\sigma(I)$][a]	0.0747	0.0645
wR_2 (all data)[b]	0.2230	0.1732
$\Delta\rho_{min,\ max}$ / e Å^{-3}	-0.254, 0.392	-0.285, 0.515

[a] $R_1 = \Sigma||F_0| - |F_c||/\Sigma|F_0|$. [b] $wR_2 = [\Sigma w(F_0^2 - F_c^2)^2/\Sigma w(F_0^2)^2]^{1/2}$.

8. DFT calculations of a fluorophore moiety

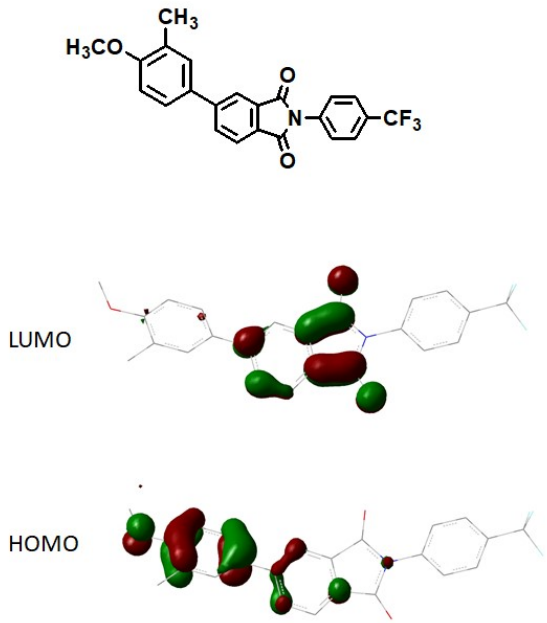

Fig. S8 Frontier orbitals of the fluorophore moiety (B3LYP/6-31G(d)).

Table S6. DFT and TD-DFT calculation data for the $S_0 \rightarrow S_1$ transition of the fluorophore moiety (B3LYP/6-31G(d)).

HOMO level	−6.02 eV
LUMO level	−2.38 eV
excitation energy (E_{ex})	3.182 eV
wavelength calculated from the E_{ex} value (λ_{ex})	389.6 nm
oscillator strength (f)	0.1787
configuration	HOMO→LUMO (0.686) HOMO−1→LUMO (−0.144)

Table S7. Cartesian coordinate (in Å) of the fluorophore moiety (B3LYP/6-31G(d)).

No	atom	x	y	z
1	C	-4.3579374	-5.4839233	0.2898403
2	C	-2.9722352	-5.5013462	0.1426760
3	C	-2.2532606	-4.3179714	0.0391725
4	C	-2.9670748	-3.1180324	0.0934390
5	C	-4.3722492	-3.0809527	0.2394591
6	C	-5.0758554	-4.3014710	0.3373962
7	C	-4.8455561	-6.8885798	0.3594440
8	C	-2.5106419	-6.9109611	0.1230606
9	H	-1.1729815	-4.3281789	-0.0677700
10	H	-2.4233348	-2.1795172	0.0468613
11	H	-6.1575666	-4.3194759	0.4216287
12	O	-5.9867557	-7.2819164	0.4806881
13	O	-1.3785556	-7.3336217	0.0154806
14	C	-3.6994975	-9.1287715	0.2841255
15	C	-2.6635963	-9.8279813	0.9188068
16	C	-4.7462425	-9.8329700	-0.3270915
17	C	-2.6771630	-11.2195700	0.9360695
18	H	-1.8472631	-9.2874447	1.3789313
19	C	-4.7571955	-11.2241379	-0.2927836
20	H	-5.5488671	-9.2957770	-0.8145505
21	C	-3.7232668	-11.9231613	0.3346906
22	H	-1.8686211	-11.7586661	1.4182661
23	H	-5.5665952	-11.7669394	-0.7694034
24	N	-3.6869297	-7.7061461	0.2570900
25	C	-3.7666514	-13.4239060	0.4128264
26	F	-4.3990999	-13.9662770	-0.6520489
27	F	-2.5277896	-13.9622325	0.4676844
28	F	-4.4263866	-13.8497760	1.5163984
29	C	-5.0944239	-1.7886713	0.2897985
30	C	-4.6717295	-0.6862257	-0.4790515
31	C	-6.2219706	-1.6204172	1.1033441
32	C	-5.3277796	0.5399813	-0.4556016
33	H	-3.8184254	-0.7978227	-1.1432095
34	C	-6.9002767	-0.4025755	1.1540319
35	H	-6.5639767	-2.4372898	1.7322598

36	C	-6.4592076	0.6751685	0.3797827
37	H	-7.7615027	-0.3034097	1.8045675
38	O	-7.0548888	1.9013153	0.3588696
39	C	-8.2064226	2.1116462	1.1620958
40	H	-8.5114564	3.1439763	0.9822988
41	H	-9.0236522	1.4361787	0.8778177
42	H	-7.9824412	1.9797175	2.2286183
43	C	-4.8714915	1.7044879	-1.2974613
44	H	-5.6622595	2.0359194	-1.9807631
45	H	-4.6161492	2.5697319	-0.6742368
46	H	-3.9927064	1.4360763	-1.8914131

9. TG-DTA data of *cis-syn*-1

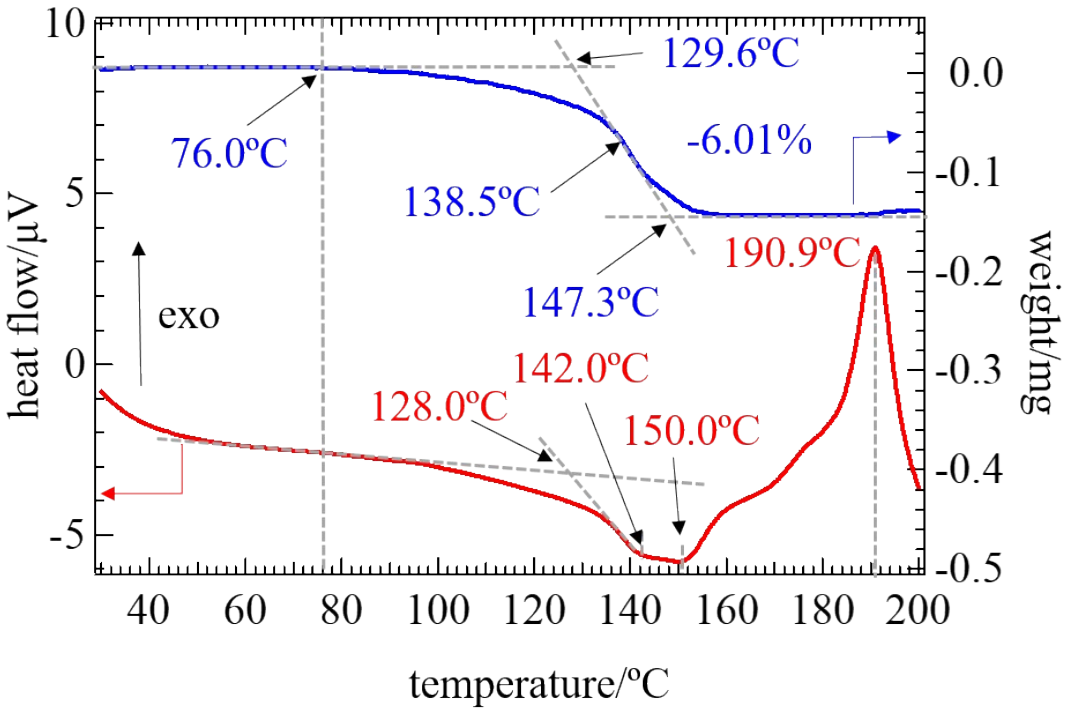

Fig. S9 TG-DTA diagram of *cis-syn*-**1** heated at elevated temperature from 30 to 200°C at 10 °C min^{-1} rate in an opened alumina pan under N_2 gas flow (300 mL min^{-1}). The sample weight was 2.49 mg.

10. Observation of a movement of a heated single crystal of *cis-syn*-1

A Pyrex glass plate with a hole (φ 4 mm, thickness 2 mm, 10 × 10 mm) at the center was superimposed on a Pyrex glass plate (thickness 2 mm, 10 × 10 mm). Then, single crystals of *cis-syn*-**1** were taken in the center hole and covered with another Pyrex glass plate (thickness 2 mm, 10 × 10 mm). The set of the sample glass plates was placed on the heating stage of an optical microscope. Magnified images of the crystals heated from 30 °C to 130 °C were obtained with a digital camera of the optical microscope, to show the morphological changes of the crystals (Figure S10). By replacing the digital camera to a sCMOS camera, magnified images of the heated crystals to show CL emissions were obtained (Figure S11). The digital camera images of the heated single crystals showed their deformations in the range of 90-100 °C. The sCMOS camera images of the heated single crystals indicate that CL in the crystals was observed over 90 °C with showing deformations around at 100 °C.

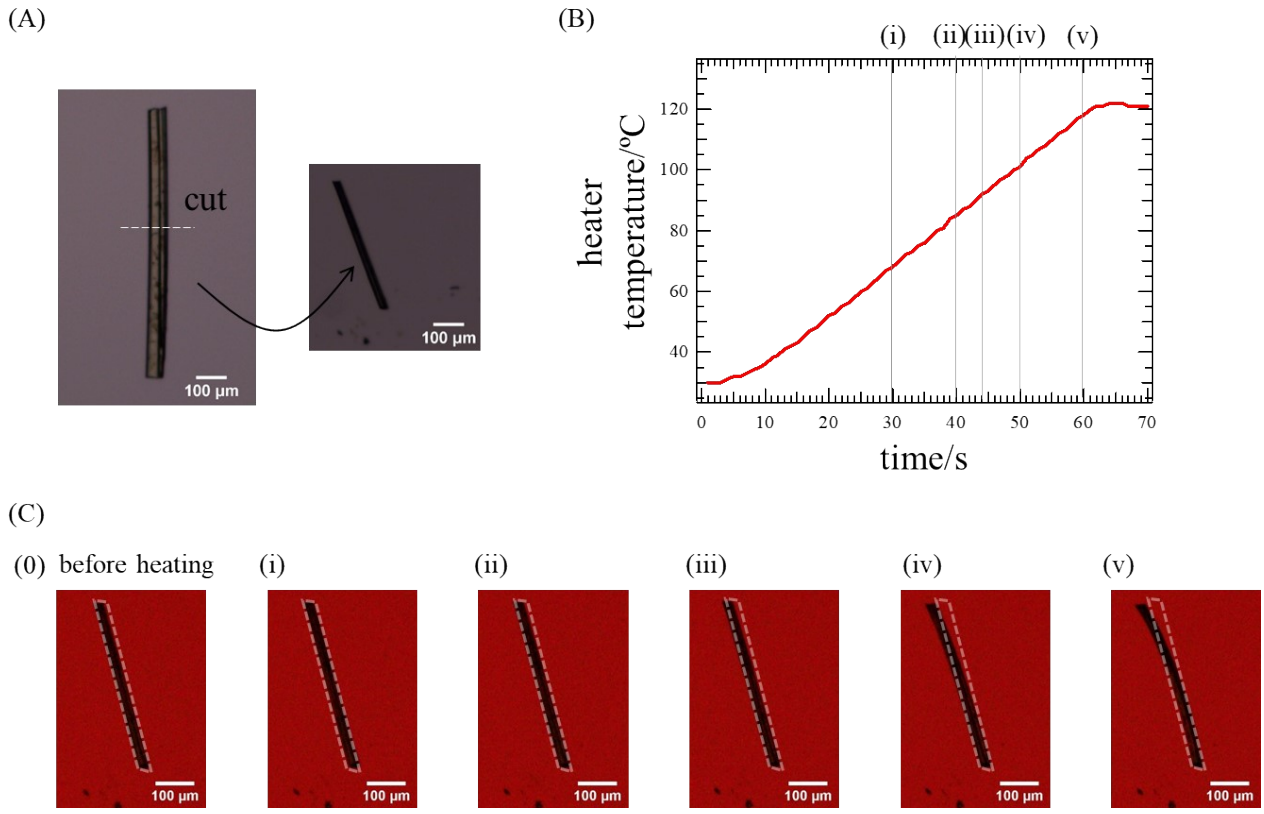

Fig. S10 (A) Photographs of a single crystal of *cis-syn*-**1** before and after heating. The size of the crystal was adjusted by cutting to 28.3 × 57.9 × 441.3 μm. (B) A heating condition at elevated temperature at 100 °C/min. (C) Photographs to show morphological changes of the single crystal under heating. Because *cis-syn*-**1** is light-sensitive, an optical filter was used to cut off transmitted light in the short wavelength region below 560 nm.

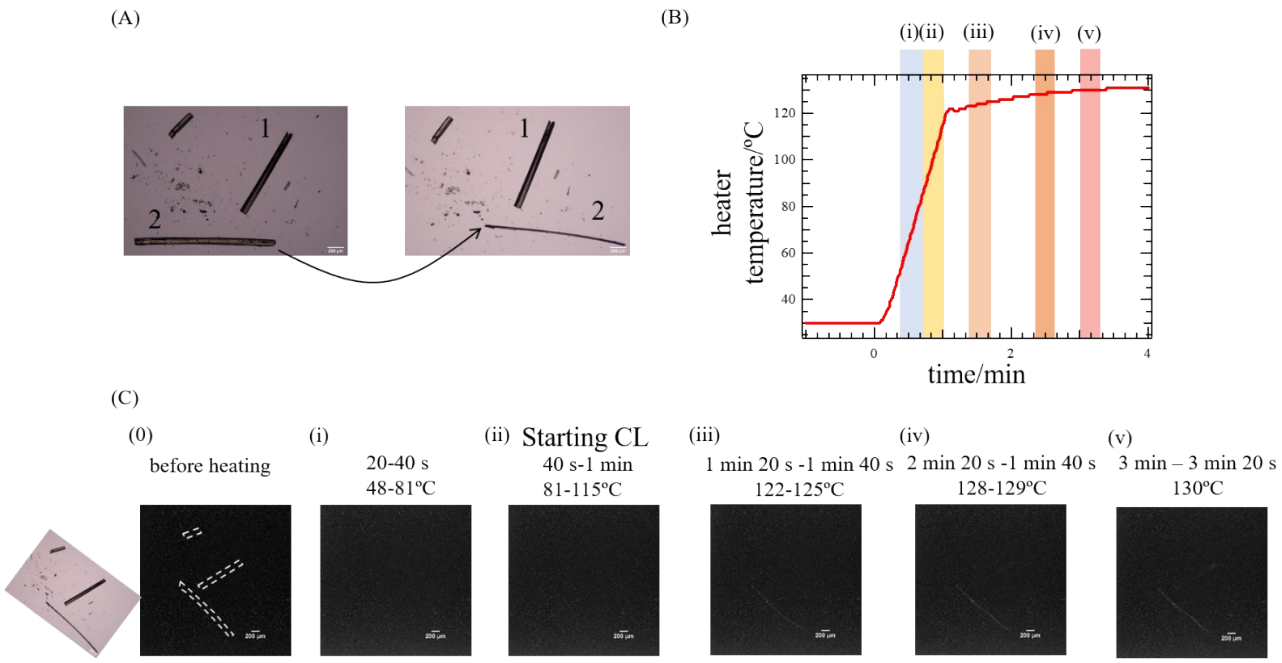

Fig. S11 (A) Photographs of single crystals of *cis-syn*-**1**. The sizes of crystals were 20.0 × 87.6 × 1114.1 μm for crystal 1 and 26.4 × 86.8 × 1699.8 μm for crystal 2. (B) A heating condition of the single crystals. (C) sCMOS camera images of the crystals including crystal 1 (thickness 20.0 μm) and crystal 2 (thickness 86.8 μm) under heating.

11. ^{1}H- and ^{13}C-NMR spectra

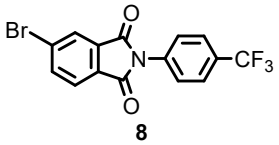

8

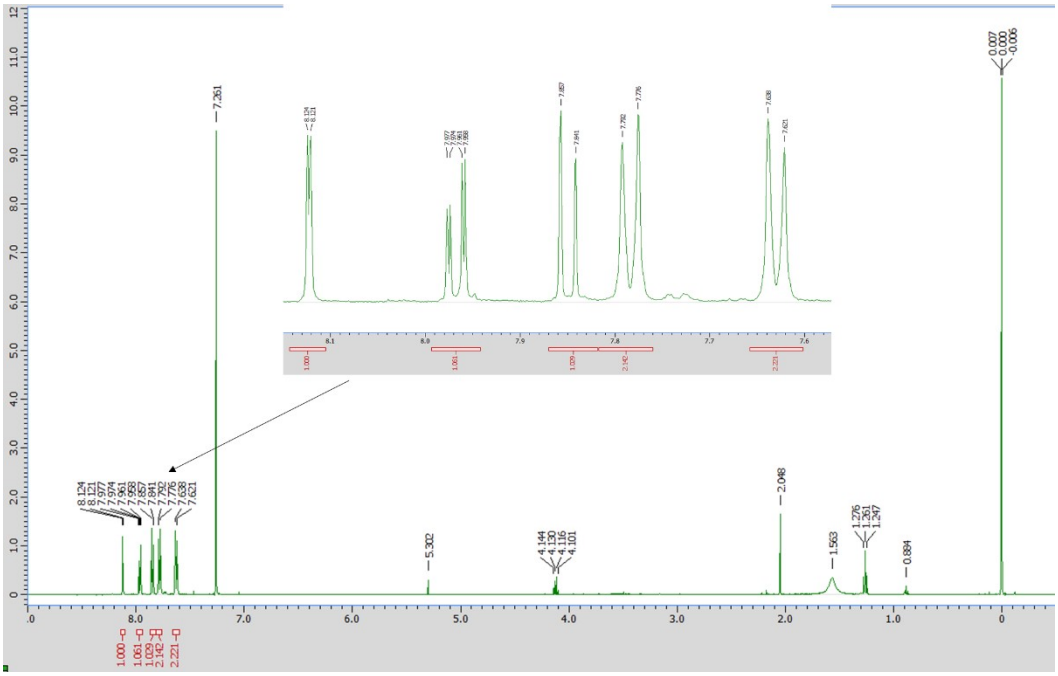

Fig. S12 ^{1}H NMR spectrum of 5-bromo-2-[4-(trifluoromethyl)phenyl]isoindoline-1,3-dione (**8**) in $CDCl_3$.

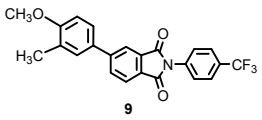

9

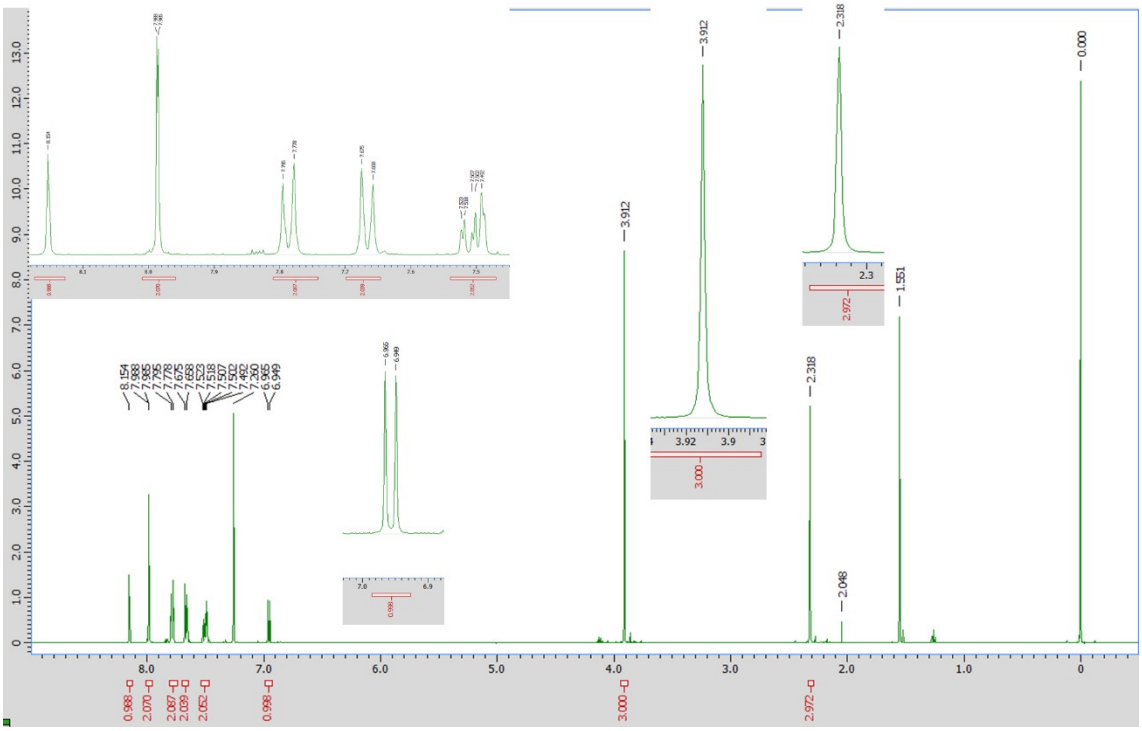

Fig. S13 ^{1}H NMR spectrum of 5-(3-methyl-4-methoxyphenyl)-2-[4-(trifluoromethyl)phenyl]isoindoline-1,3-dione (**9**) in $CDCl_3$.

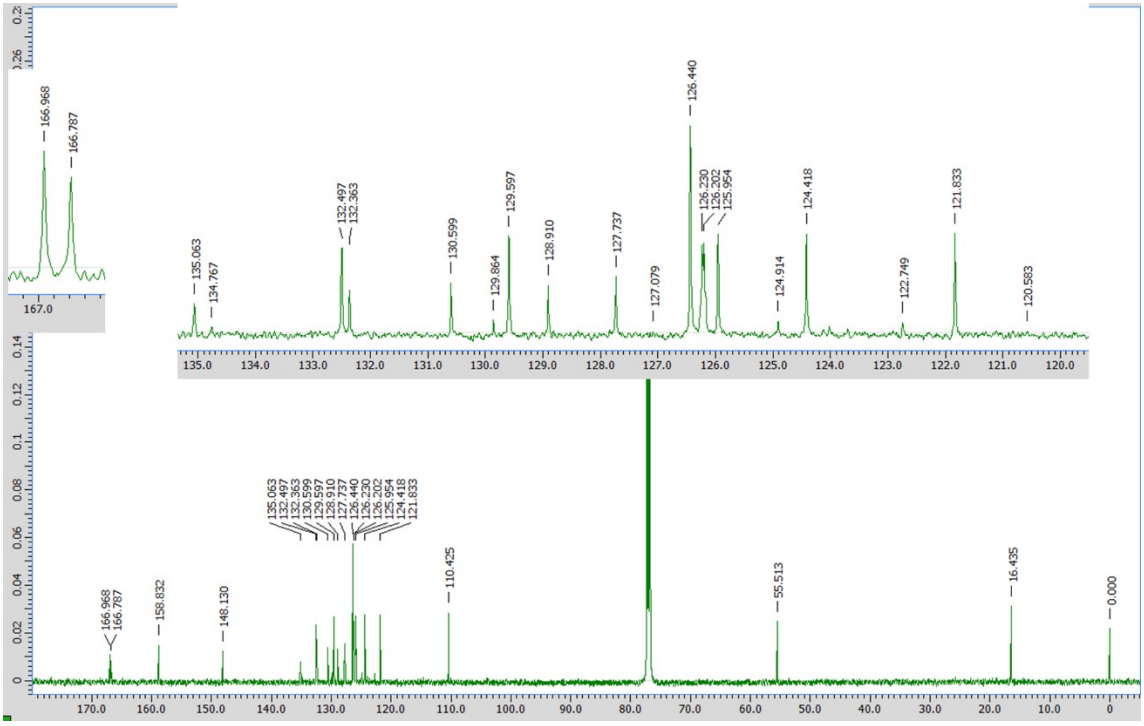

Fig. S14 ^{13}C NMR spectrum of 5-(3-methyl-4-methoxyphenyl)-2-[4-(trifluoromethyl)phenyl]isoindoline-1,3-dione (**9**) in $CDCl_3$.

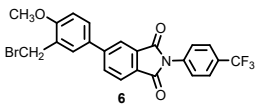

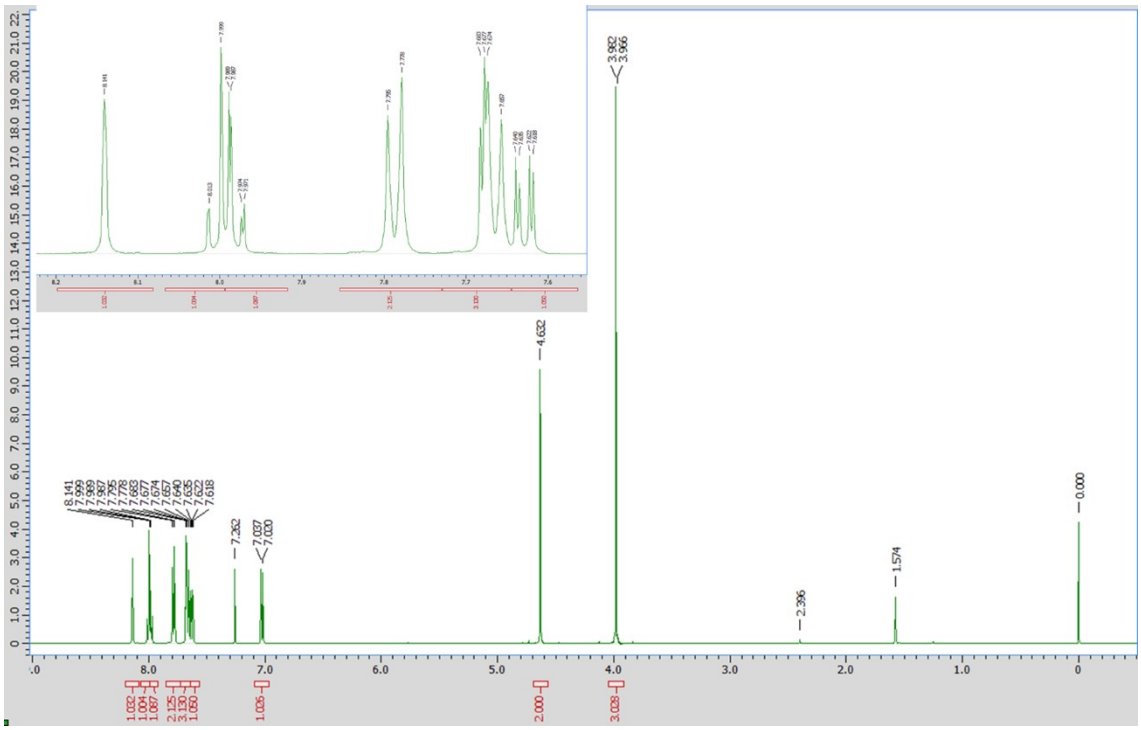

Fig. S15 ^{1}H NMR spectrum of 5-(3-bromomethyl-4-methoxyphenyl)-2-[4-(trifluoromethyl)phenyl]isoindoline-1,3-dione (**6**) in $CDCl_3$.

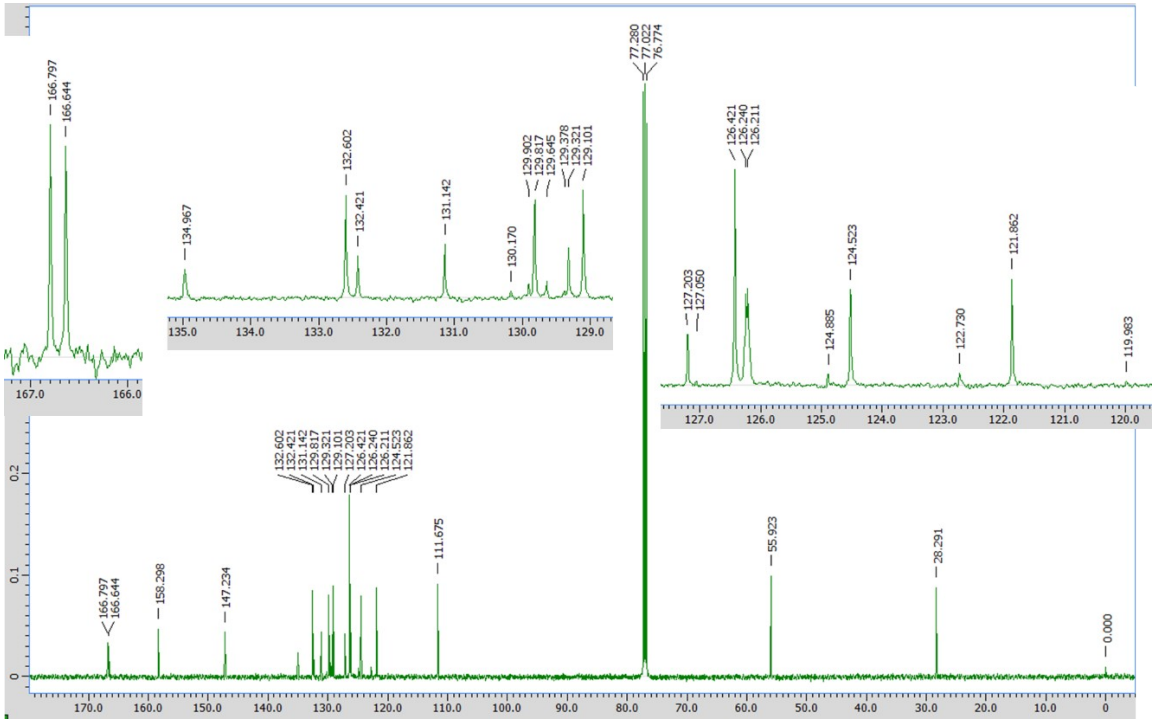

Fig. S16 ^{13}C NMR spectrum of 5-(3-bromomethyl-4-methoxyphenyl)-2-[4-(trifluoromethyl)phenyl]isoindoline-1,3-dione (**6**) in $CDCl_3$.

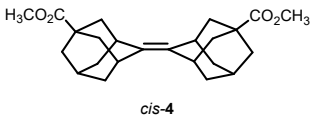

cis-**4**

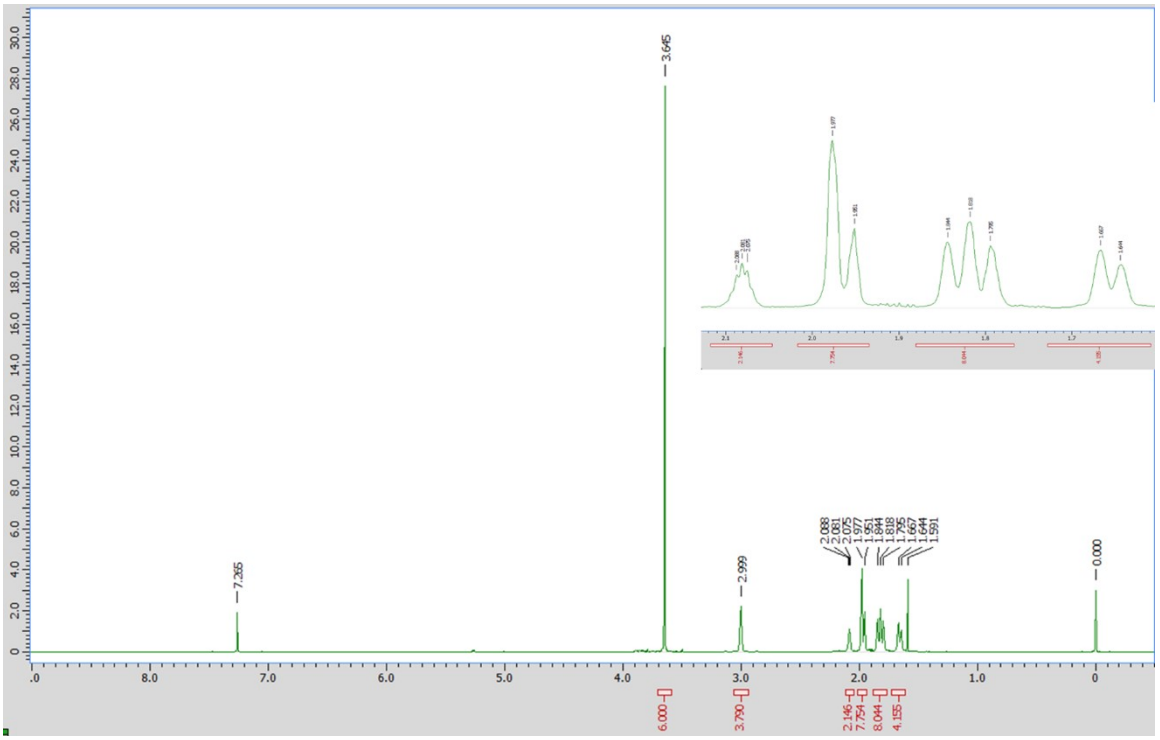

Fig. S17 ^{1}H NMR spectrum of *cis*-5,5'-dicarbomethoxyadamantylideneadamantane (*cis*-**4**) in $CDCl_3$.

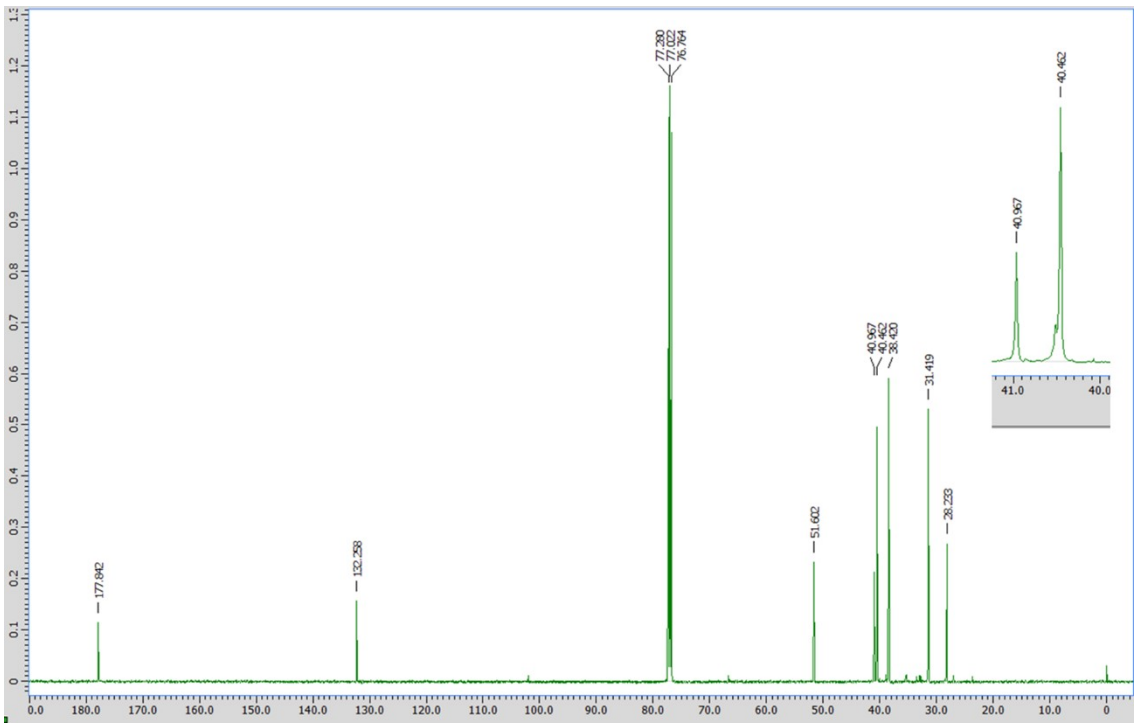

Fig. S18 ^{13}C NMR spectrum of *cis*-5,5'-dicarbomethoxyadamantylideneadamantane (*cis*-**4**) in $CDCl_3$.

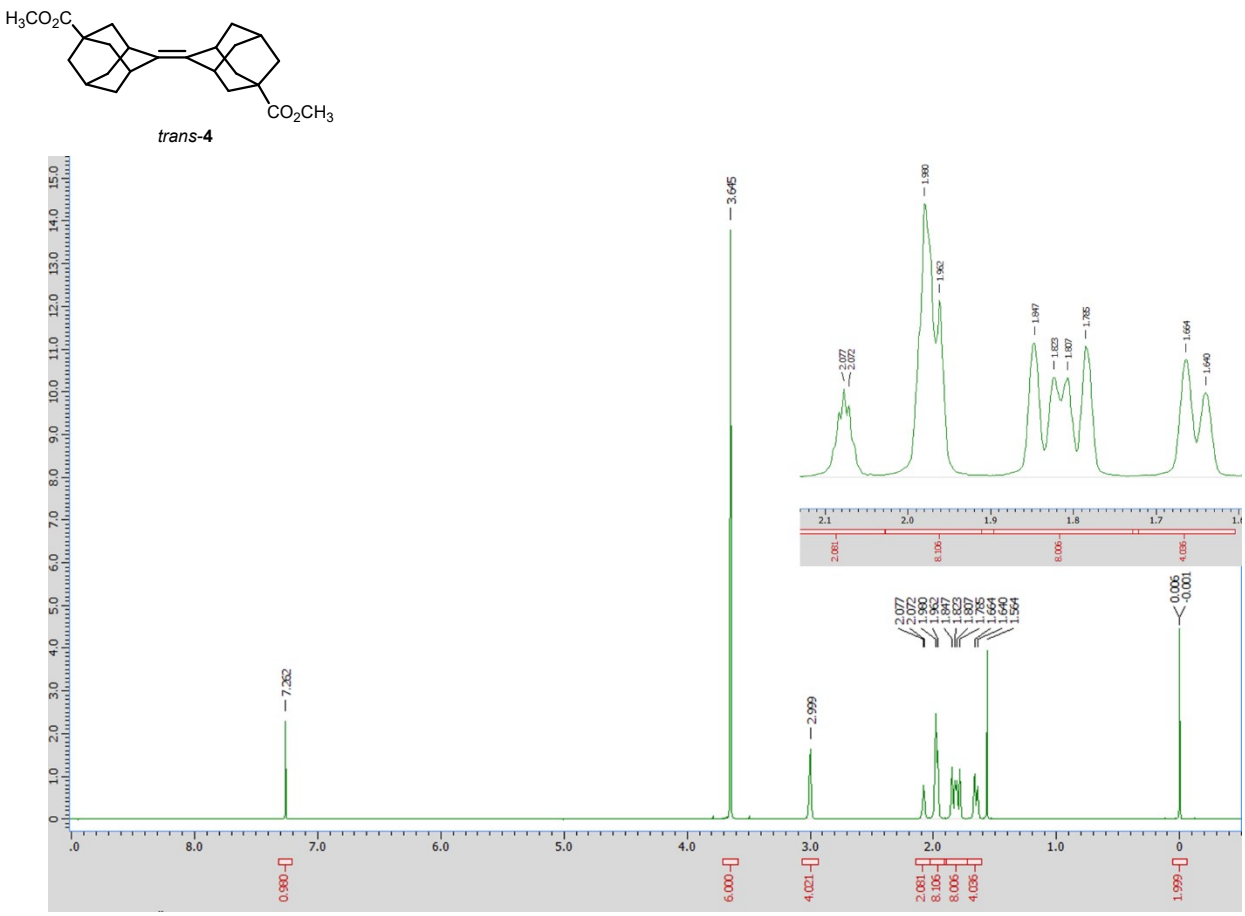

Fig. S19 ^{1}H NMR spectrum of *trans*-5,5'-dicarbomethoxyadamantylideneadamantane (*trans*-**4**) in $CDCl_3$.

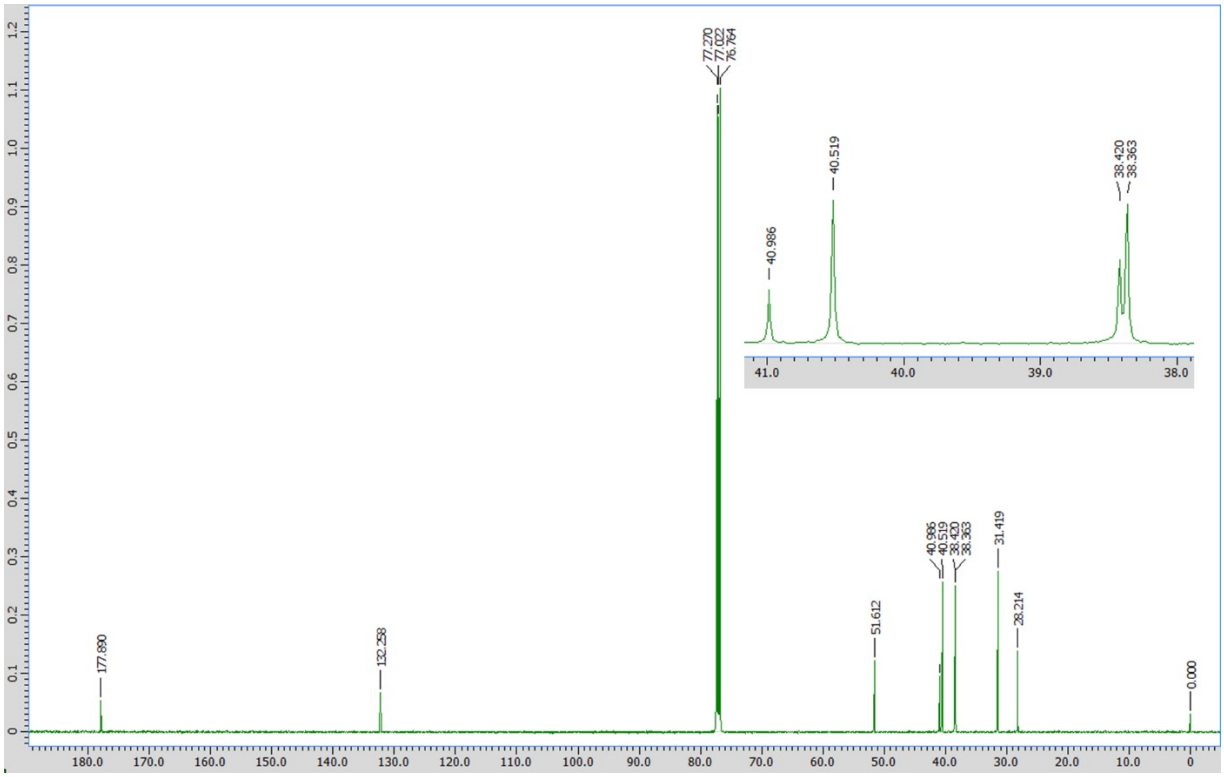

Fig. S20 ^{13}C NMR spectrum of *trans*-5,5'-dicarbomethoxyadamantylideneadamantane (*trans*-**4**) in

$CDCl_3$.

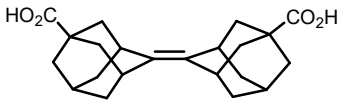

cis-**5**

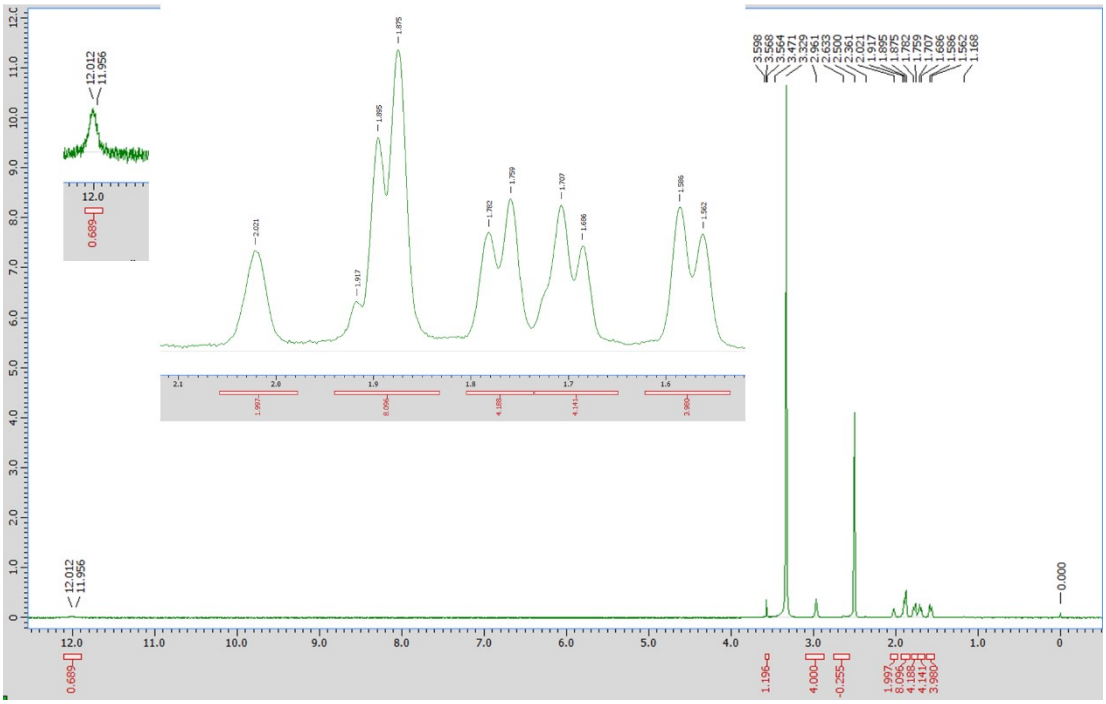

Fig. S21 ^{1}H NMR spectrum of *cis*-5,5'-dicarboxyadamantylideneadamantane (*cis*-**5**) in DMSO-d_6.

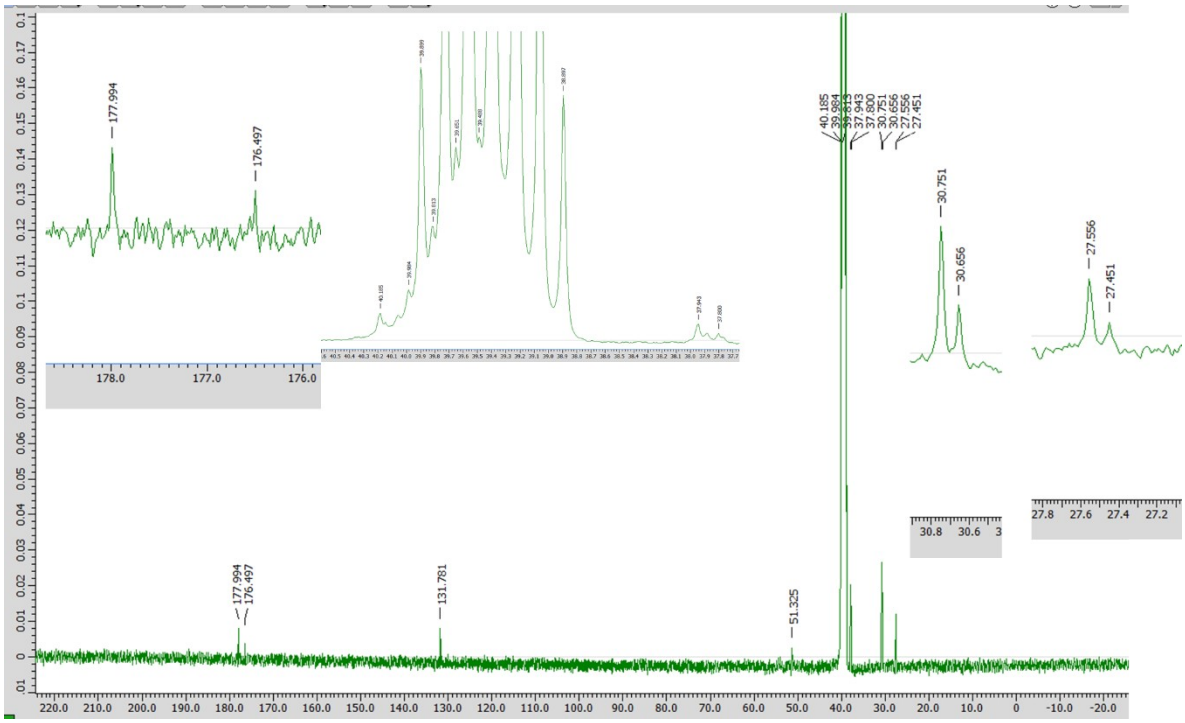

Fig. S22 ^{13}C NMR spectrum of *cis*-5,5'-dicarboxyadamantylideneadamantane (*cis*-**5**) in DMSO-d_6.

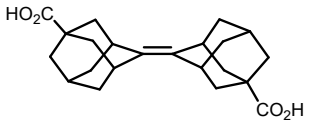

trans-**5**

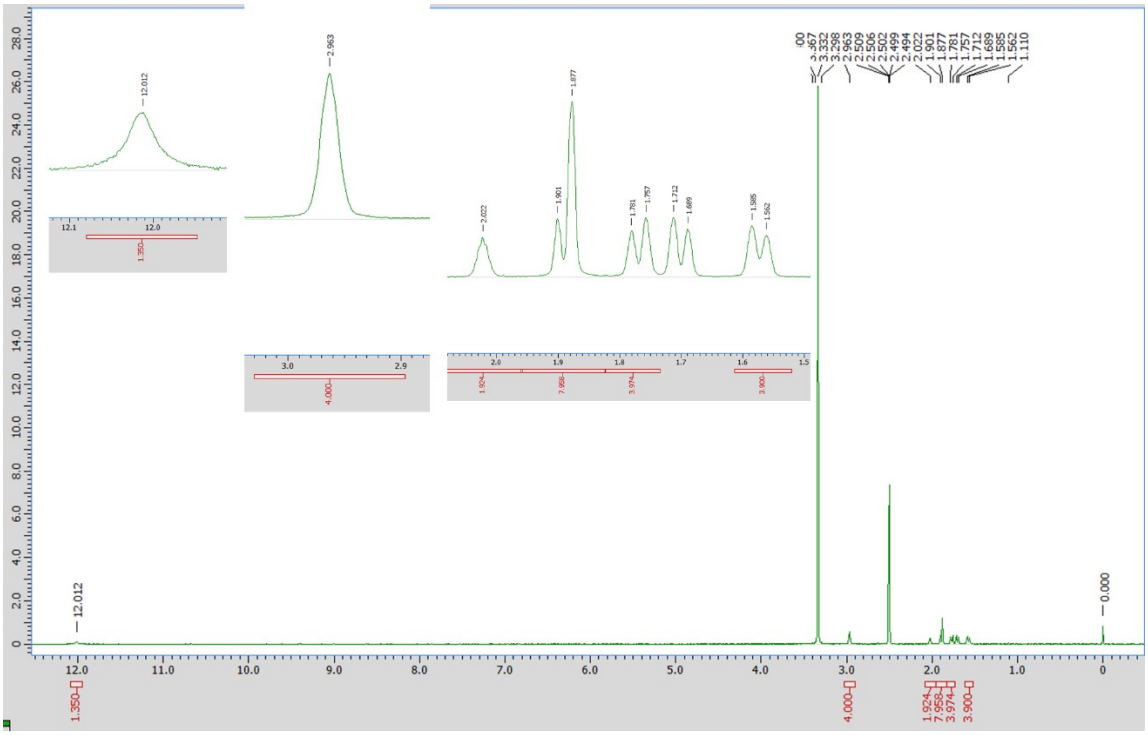

Fig. S23 ^{1}H NMR spectrum of *trans*-5,5'-dicarboxyadamantylideneadamantane (*trans*-**5**) in DMSO-d_6.

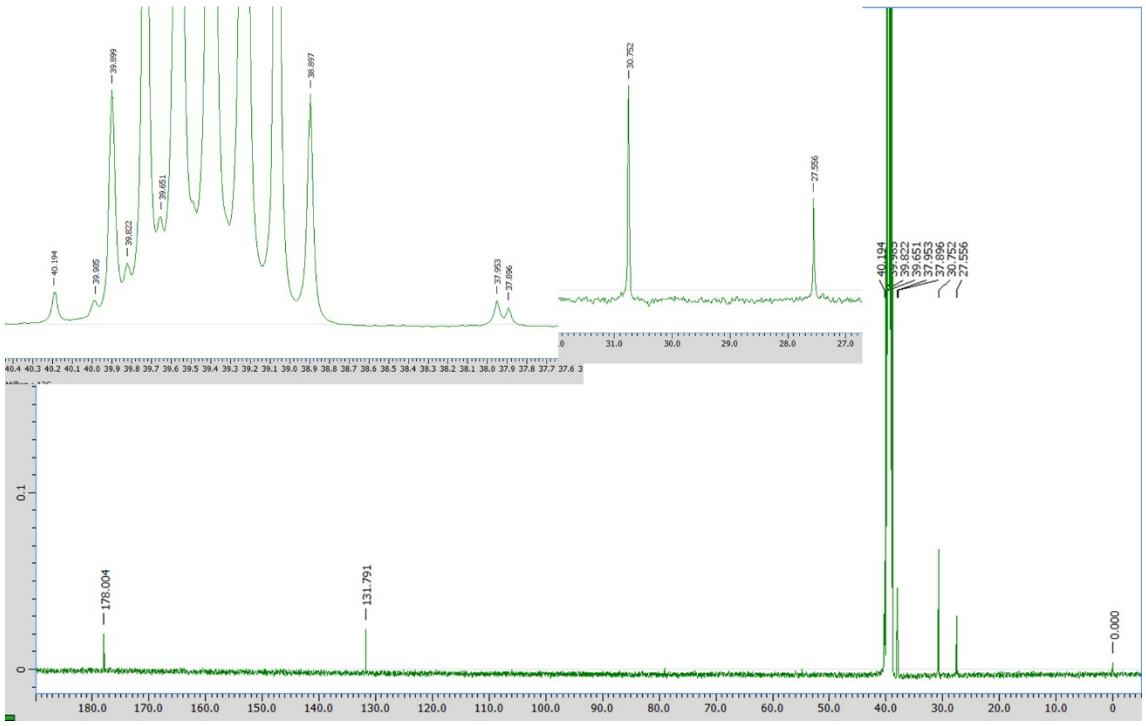

Fig. S24 ^{13}C NMR spectrum of *trans*-5,5'-dicarboxyadamantylideneadamantane (*trans*-**5**) in

DMSO-d_6.

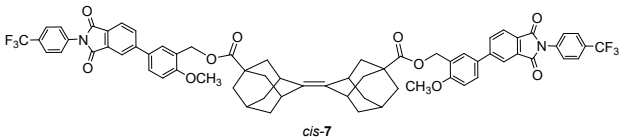

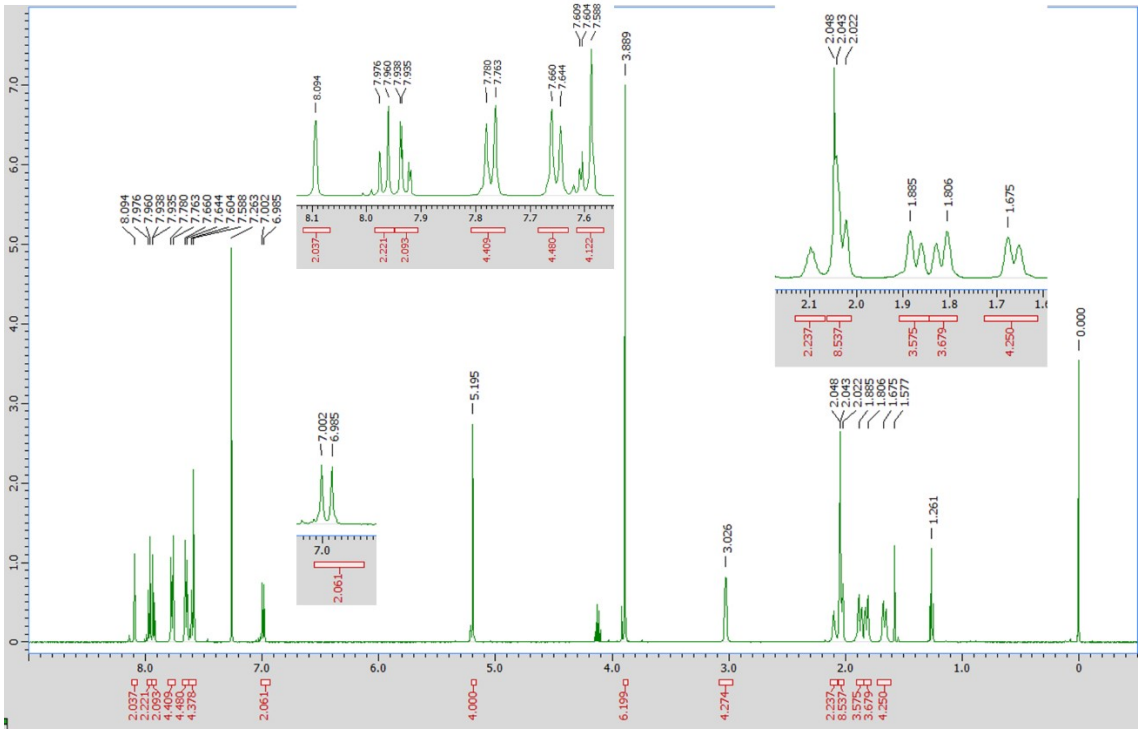

Fig. S25 ^{1}H NMR spectrum of *cis*-5,5'-di{1-methoxy-4-[4-(trifluoromethyl)phenyl]isoindoline-1,3-dionylbenzyloxycarbonyl}adamantylideneadamantane (*cis*-**7**) in $CDCl_3$.

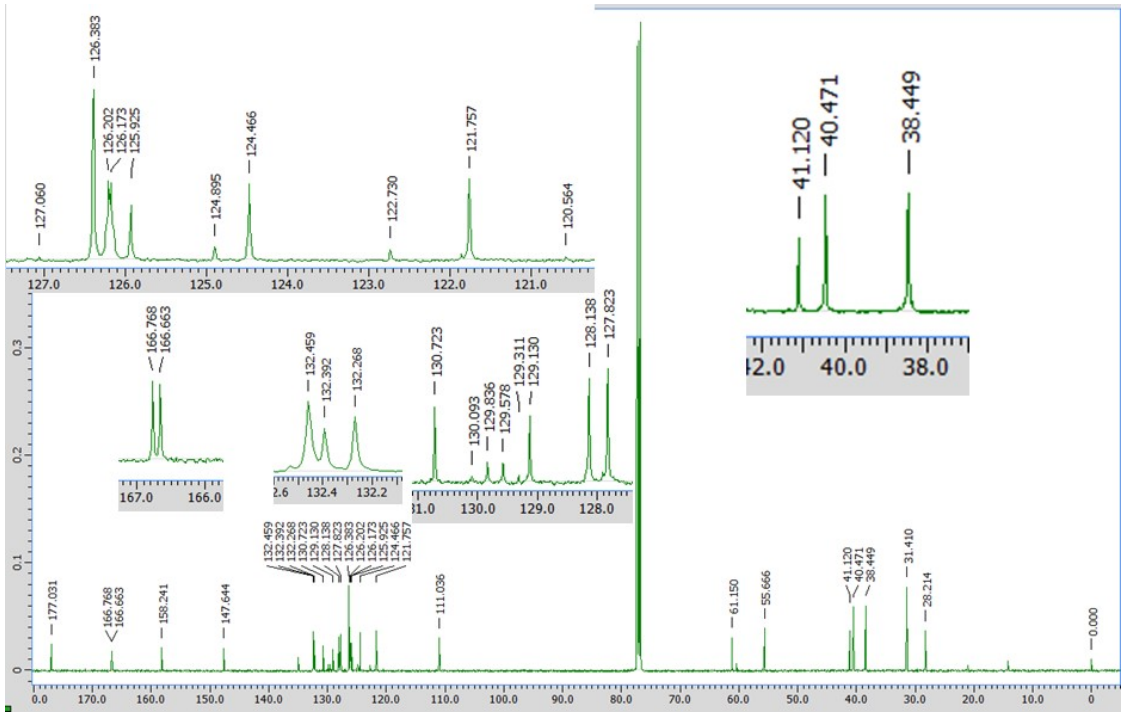

Fig. S26 ^{13}C NMR spectrum of *cis*-5,5'-di{1-methoxy-4-[4-(trifluoromethyl)phenyl]isoindoline-

1,3-dionylbenzyloxycarbonyl}adamantylideneadamantane (*cis*-**7**) in $CDCl_3$.

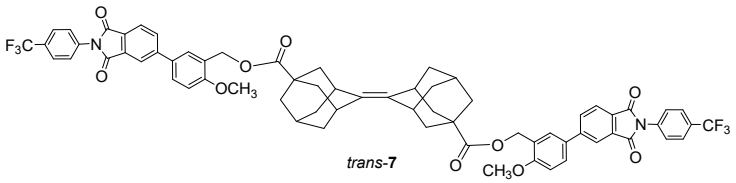

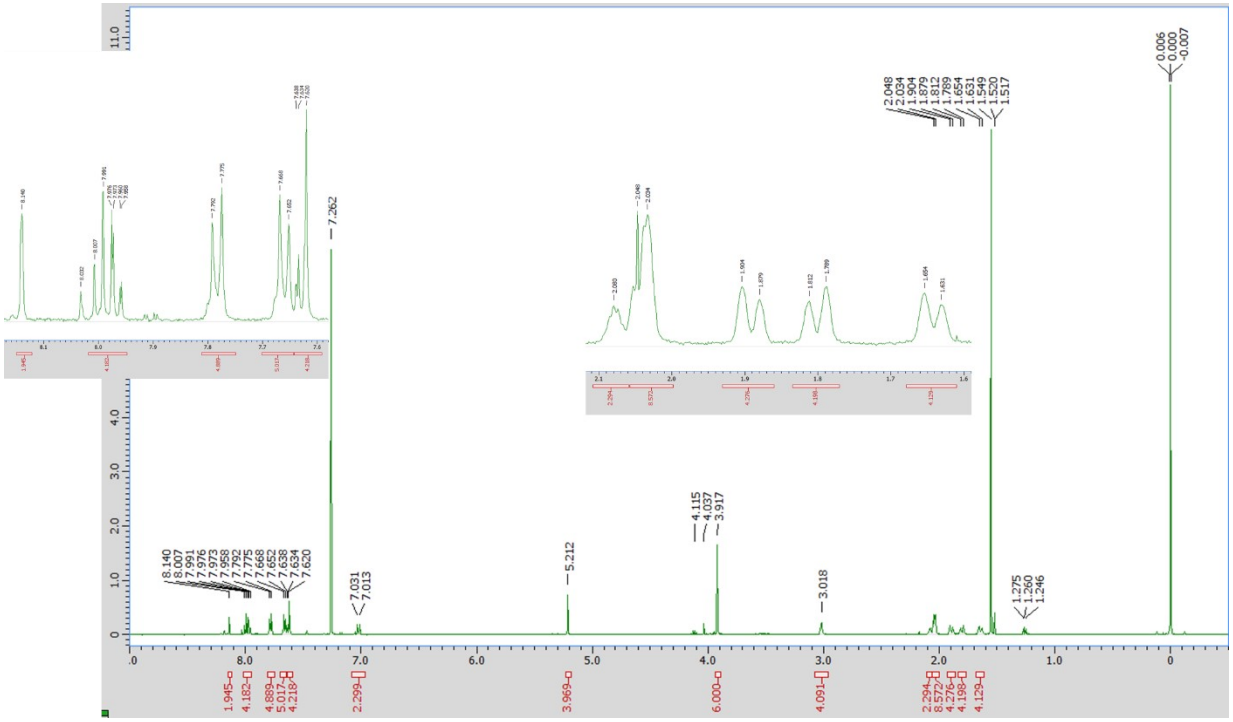

Fig. S27 ^{1}H NMR spectrum of *trans*-5,5'-di{1-methoxy-4-[4-(trifluoromethyl)phenyl]isoindoline-1,3-dionylbenzyloxycarbonyl}adamantylideneadamantane (*trans*-**7**) in $CDCl_3$.

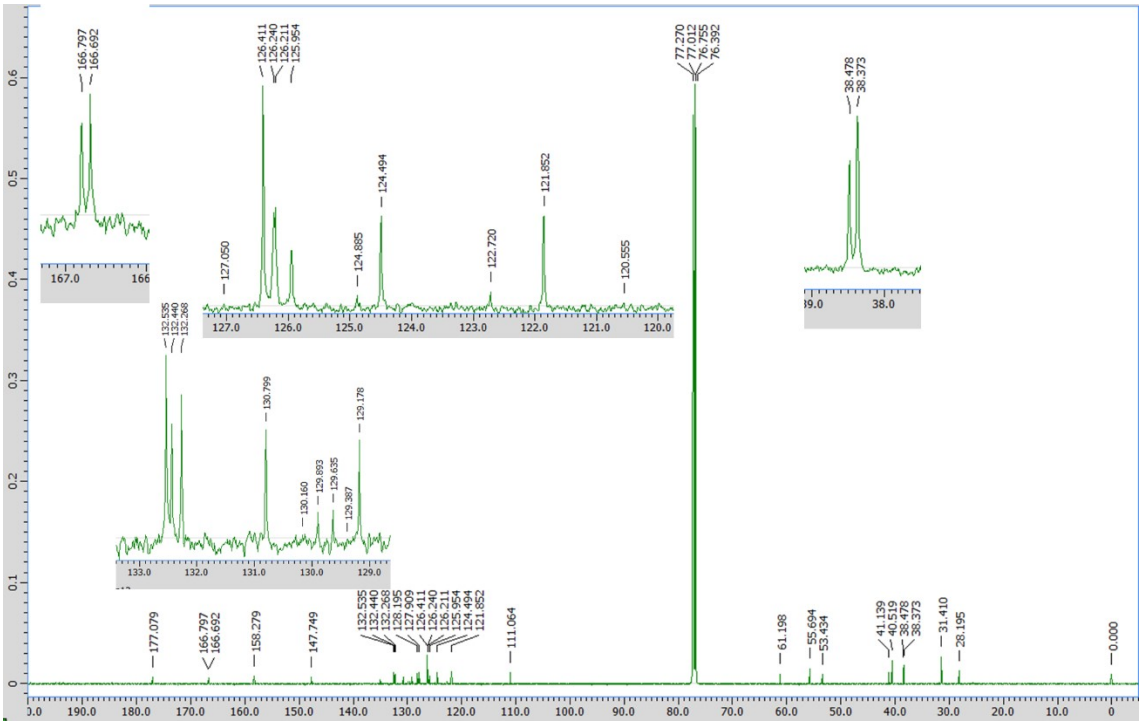

Fig. S28 ^{13}C NMR spectrum of *trans*-5,5'-di{1-methoxy-4-[4-(trifluoromethyl)phenyl]isoindoline-

1,3-dionylbenzyloxycarbonyl}adamantylideneadamantane (*trans*-**7**) in $CDCl_3$.

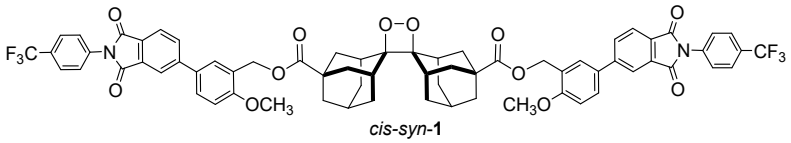

cis-syn-**1**

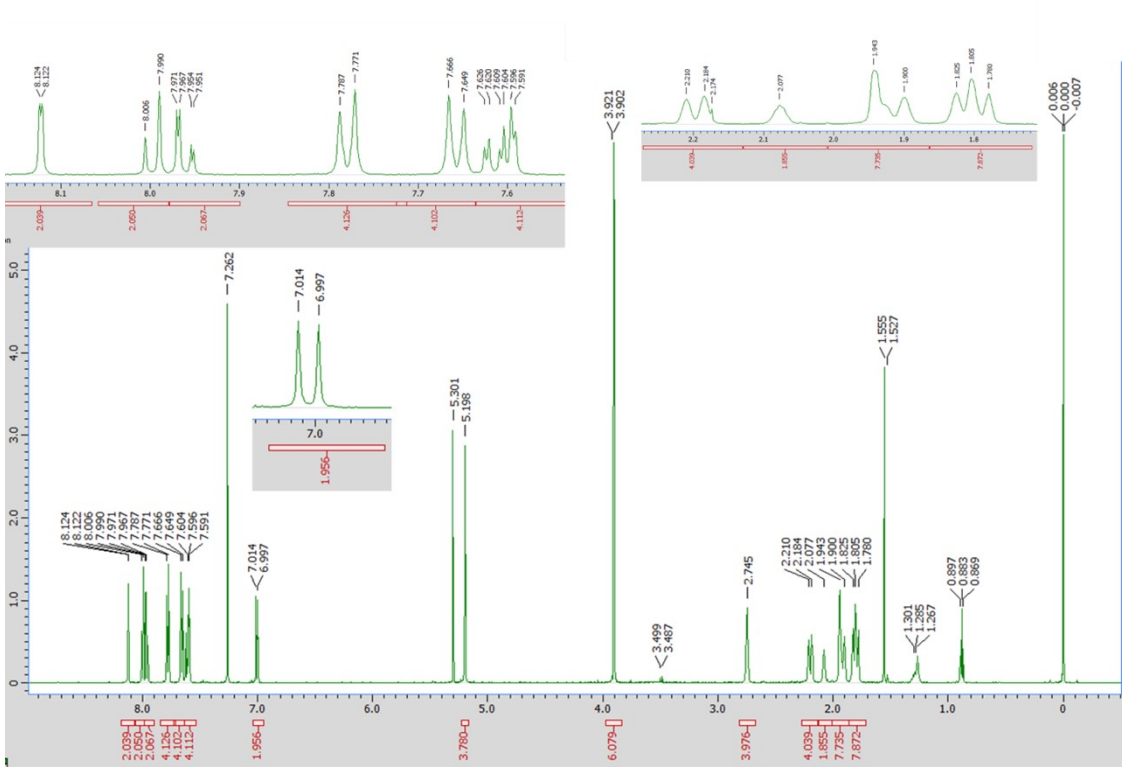

Fig. S29 ^{1}H NMR spectrum of *cis-syn*-5,5'-di{1-methoxy-4-[4-(trifluoromethyl)phenyl]isoindoline-1,3-dionylbenzyloxycarbonyl}adamantylideneadamantane 1,2-dioxetane (*cis-syn*-**1**) in $CDCl_3$.

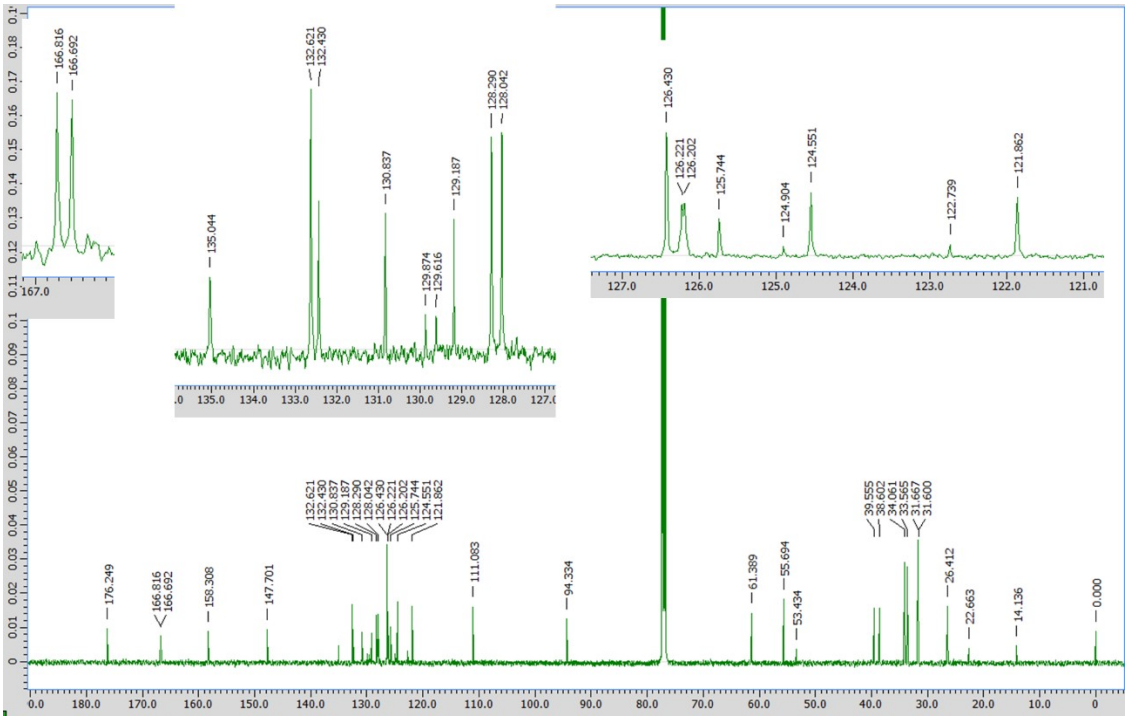

Fig. S30 ^{13}C NMR spectrum of *cis-syn*-5,5'-di{1-methoxy-4-[4-(trifluoromethyl)phenyl]isoindoline-1,3-dionylbenzyloxycarbonyl}adamantylideneadamantane 1,2-dioxetane (*cis-syn*-**1**) in $CDCl_3$.

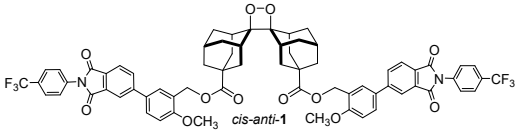

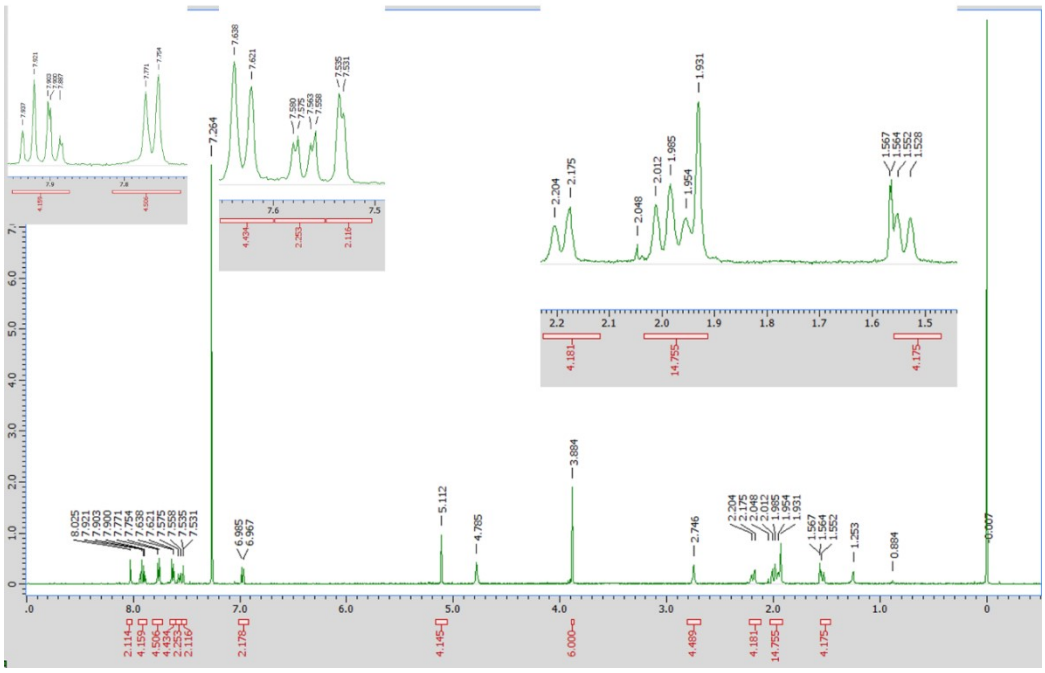

Fig. S31 ^{1}H NMR spectrum of *cis-anti*-5,5'-di{1-methoxy-4-[4-(trifluoromethyl)phenyl]-isoindoline-1,3-dionylbenzyloxycarbonyl}adamantylideneadamantane 1,2-dioxetane (*cis-anti*-**1**) in $CDCl_3$ containing D_2O.

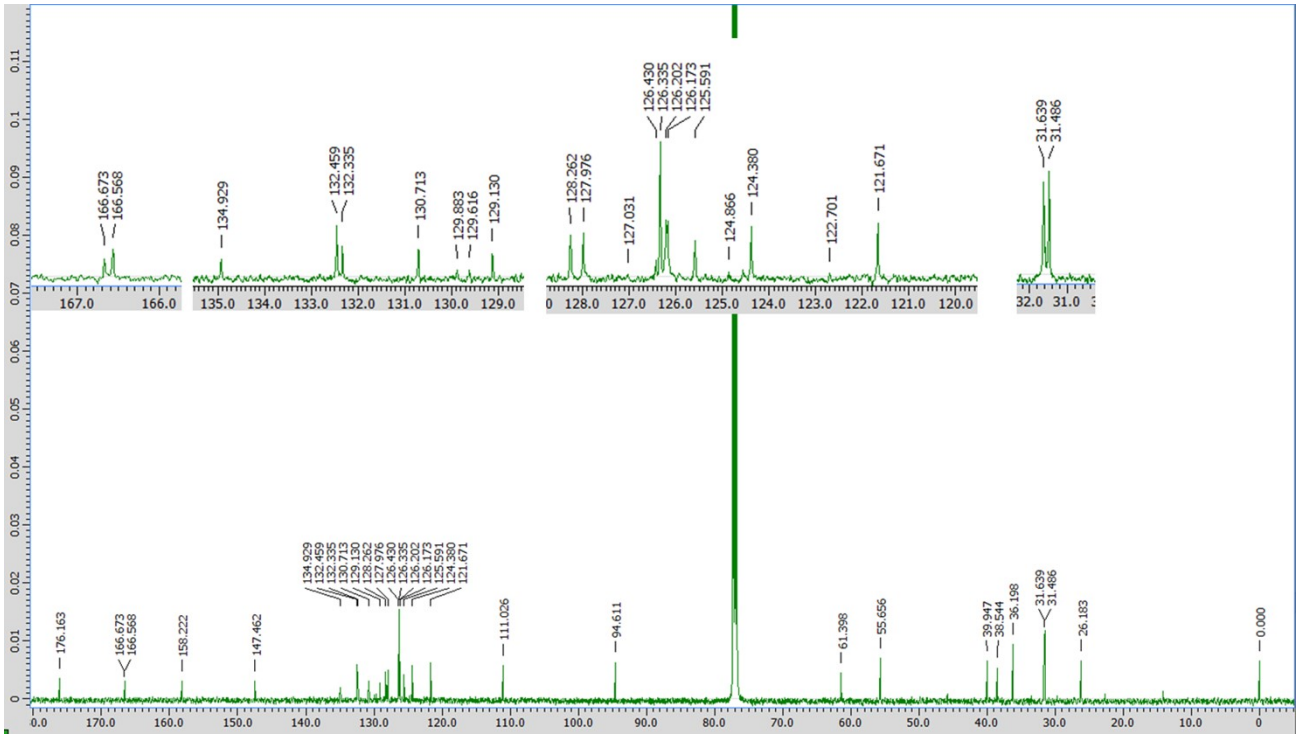

Fig. S32 ^{13}C NMR spectrum of *cis*-*anti*-5,5'-di{1-methoxy-4-[4-(trifluoromethyl)phenylisoindoline-1,3-dionyl]benzyl}calboxyadamantylideneadamantane 1,2-dioxetane (*cis*-*anti*-**1**) in $CDCl_3$.

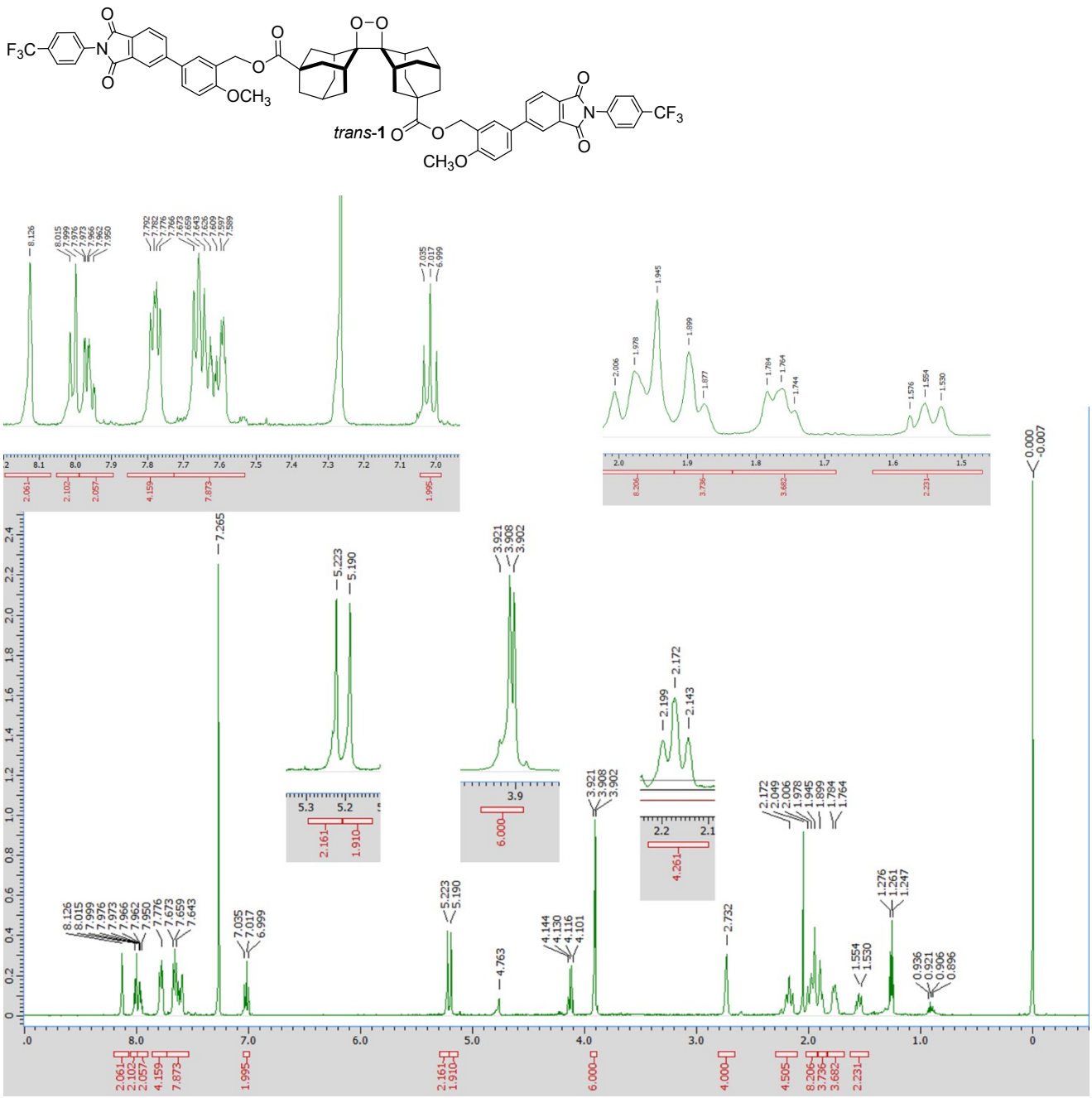

Fig. S33 ^{1}H NMR spectrum of *trans*-5,5'-di{1-methoxy-4-[4-(trifluoromethyl)phenyl]isoindoline-1,3-dionylbenzyloxycarbonyl}adamantylideneadamantane 1,2-dioxetane (*trans*-**1**) in $CDCl_3$ containing D_2O.

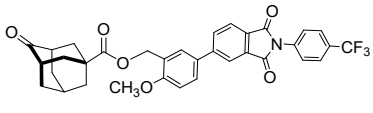

2

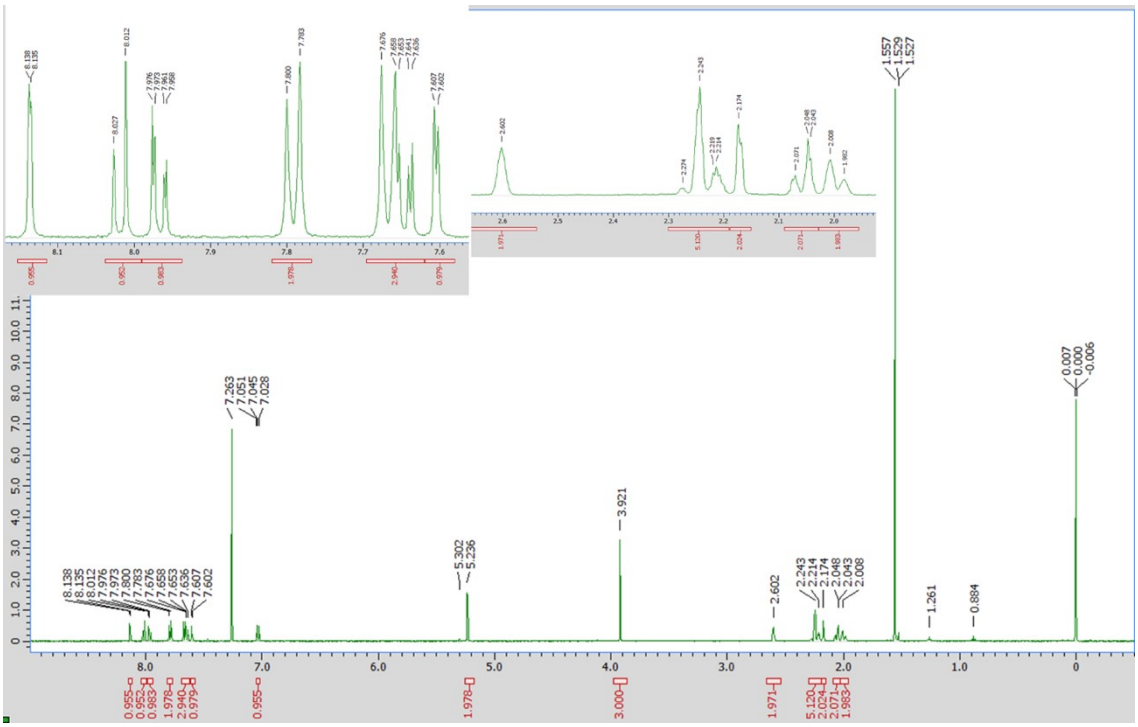

Fig. S34 ^{1}H NMR spectrum of 5-{1-methoxy-4-[4-(trifluoromethyl)phenyl]isoindoline-1,3-dionylbenzyloxycarbonyl}-2-adamantanone (**2**) in $CDCl_3$.

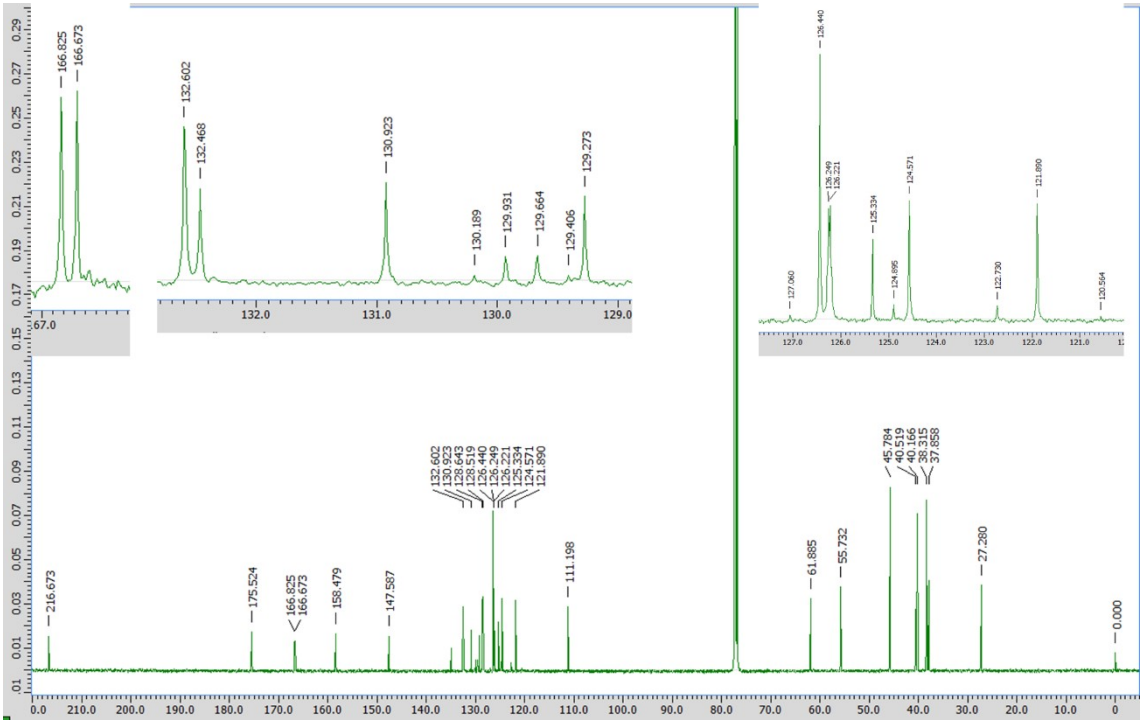

Fig. S35 ^{13}C NMR spectrum of 5-{1-methoxy-4-[4-(trifluoromethyl)phenyl]isoindoline-1,3-dionylbenzyloxycarbonyl}-2-adamantanone (**2**) in $CDCl_3$.

References

1. W. Kabsch*, Acta Crystallogr. Sect. D* **2010**, *66*, 125-132.
2. O. V. Dolomanov, L. J. Bourhis, R. J. Gildea, J. A. K. Howard and H. Puschmann, *J. Appl. Crystallogr.* **2009**, *42*, 339–341.
3. G. M. Sheldrick, *Acta Crystallogr. Sect. A* **2015**, *A71*, 3−8.
4. G. M. Sheldrick, *Acta Crystallogr., Sect. C* **2015**, *71*, 3−8.
5. A. L. Spek, *Acta Crystallogr. Sect. C* **2015**, *71*, 9–18.
6. M. J. Frisch, G. W. Trucks, H. B. Schlegel, G. E. Scuseria, M. A. Robb, J. R. Cheeseman, G. Scalmani, V. Barone, G. A. Petersson, H. Nakatsuji, X. Li, M. Caricato, A. V. Marenich, J. Bloino, B. G. Janesko, R. Gomperts, B. Mennucci, H. P. Hratchian, J. V. Ortiz, A. F. Izmaylov, J. L. Sonnenberg, D. Williams-Young, F. Ding, F. Lipparini, F. Egidi, J. Goings, B. Peng, A. Petrone, T. Henderson, D. Ranasinghe, V. G. Zakrzewski, J. Gao, N. Rega, G. Zheng, W. Liang, M. Hada, M. Ehara, K. Toyota, R. Fukuda, J. Hasegawa, M. Ishida, T. Nakajima, Y. Honda, O. Kitao, H. Nakai, T. Vreven, K. Throssell, J. A. Montgomery, Jr., J. E. Peralta, F. Ogliaro, M. J. Bearpark, J. J. Heyd, E. N. Brothers, K. N. Kudin, V. N. Staroverov, T. A. Keith, R. Kobayashi, J. Normand, K. Raghavachari, A. P. Rendell, J. C. Burant, S. S. Iyengar, J. Tomasi, M. Cossi, J. M. Millam, M. Klene, C. Adamo, R. Cammi, J. W. Ochterski, R. L. Martin, K. Morokuma, O. Farkas, J. B. Foresman and D. J. Fox, *Gaussian 16*, Revision C.01, Gaussian, Inc., Wallingford CT, **2016**.
7. A. D. Becke, *J. Chem. Phys*. **1993**, *98*, 5648−5652.
8. C. T. Lee, W. T. Yang and R. G. Parr, *Phys. Rev. B* **1988**, *37*, 785−789.
9. P. J. Stephens, F. J. Devlin, C. F. Chabalowski and M. J. Frisch, *J. Phys. Chem*. **1994**, *98*, 11623−11627.
10. R. Dennington, T. A. Keith and J. M. Millam, *GaussView*, Version 6.1, Semichem Inc., Shawnee Mission KS, **2016**.
11. J. Nishida, H. Ohura, Y. Kita, H. Hasegawa, T. Kawase, N. Takada, H. Sato, Y. Sei and Y. Yamashita, *J. Org. Chem*. **2016**, *81*, 433-441.
12. W. J. Le Noble, S.Srivastava and C. K. Cheung, *J. Org. Chem*. **1983**, *48*, 1099−1101.
13. V. Barton, S. A. Ward, J. Chadwick, A. Hill and P. M. O'Neill, *J. Med. Chem*. **2010**, *53*, 4555−4559.